8-2020

Investigating the role of Quaking in antigen uptake and cross-presentation by dendritic cells

Yating Li

INVESTIGATING THE ROLE OF QUAKING IN ANTIGEN UPTAKE AND CROSS-PRESENTATION BY DENDRITIC CELLS

by

Yating Li, B.Sc.

APPROVED:

*Cassian Yee, M.D.*_____
Cassian Yee, M.D.
Advisory Professor

*Yejing Ge, Ph.D.*_____
Yejing Ge, Ph.D.

*Jian Hu, Ph.D.*_____
Jian Hu, Ph.D.

*Shao-Cong Sun, Ph.D.*_____
Shao-Cong Sun, Ph.D.

*Stephanie Watowich, Ph.D.*_____
Stephanie Watowich, Ph.D.

APPROVED:

_____
Dean, The University of Texas
MD Anderson Cancer Center UTHealth Graduate School of Biomedical Sciences

INVESTIGATING THE ROLE OF QUAKING IN ANTIGEN UPTAKE AND CROSS-PRESENTATION BY DENDRITIC CELLS

A

THESIS

Presented to the Faculty of

The University of Texas

MD Anderson Cancer Center UTHealth

Graduate School of Biomedical Sciences

in Partial Fulfillment

of the Requirements

for the Degree of

MASTER OF SCIENCE

by

Yating Li, B.Sc.

Houston, Texas

August, 2020

Acknowledgments

I would like to dedicate my acknowledgments of gratitude towards my respected and beloved supervisors, family, friends, and everyone who worked with me throughout my M.S. study.

First and foremost, I would like to express my sincere appreciation to my supervisor Dr. Cassian Yee for his valuable mentorship, guidance, encouragement, and endless support. With his trust, I was able to explore different possibilities of the project. His critical judgement and sharp perspective always made sure I was on the right path. He also helped me to establish collaborative relationships with other faculty so I could get invaluable suggestions from brilliant scientists. I am truly grateful to be his student.

I would like to extend my gratitude to Dr. Jian Hu, Dr. Yejing Ge, Dr. Stephanie Watowich and Dr. Shao-Cong Sun for serving on my advisory committee. They have been very supportive and offered me with constructive suggestions to overcome obstacles throughout the years.

I would also like to thank everyone in the Yee lab. Working with them made the graduate study very joyful (T Cells R Us!). I would love to extend my special thanks to Farah Hasan, the senior PhD student in lab. She provided me with more than scientific suggestions and technical support. Without her I would not have adapted to my graduate life so easily. In addition, I am grateful to Dr. Xin Zhou from Hu lab. He is a fantastic teacher who taught me techniques that I was not familiar with and discussing science with him has always inspiring.

Last but not least, I am greatly thankful to my family and friends, who take my up-and-downs and still give me unconditionally love and support.

Investigating the role of Quaking in antigen uptake and cross-presentation by dendritic cells

Yating Li, B.Sc.

Advisory Professor: Cassian Yee, M.D.

Dendritic cells (DCs) are considered the most potent antigen presenting cells (APC) due to their superior capability of cross-presenting exogenous antigens to $CD8^+$ T cell for strong adaptive immune responses. They internalize foreign antigens by phagocytosis, endocytosis or macropinocytosis, which are then processed in endosomal compartments and loaded onto MHC Class I molecules. However, the molecular mechanisms regulating exogenous antigen uptake and cross-presentation by DCs are not fully understood.

In this study, we discovered that an RNA-binding protein, Quaking (QKI) plays a pivotal role in antigen uptake by DCs. Our previous studies in neural stem cells and microglia have identified QKI as a novel regulator of phagosomes and endolysosomes, and knocking down of QKI significantly downregulates genes involved in phagosome maturation and endosome signaling. Furthermore, we have also shown that QKI interacts with a nuclear receptor, PPARδ, in multiple cell types. The QKI- PPARδ complex induces expression of a large set of genes associated with signaling in phagosome and endolysosome by binding to their promoter regions. Therefore, we hypothesize that in DCs, QKI and PPARδ mediated promotion of phagosome and endolysosome signaling can enhance antigen uptake and cross-presentation function of these cells.

Using human monocyte derived DCs, we found QKI and PPARδ to be significantly upregulated upon monocyte differentiation into DC *in vitro*. Our data have demonstrated that activation of QKI/PPARδ complex by PPARδ receptor agonist increases the phagocytosis activity in DCs while siRNA silencing of QKI or PPARδ impairs it. This suggests that QKI cooperates with PPARδ to enhance the antigen uptake by DCs. Our studies did not establish the role of either QKI or PPARδ in the regulation of exogenous antigen cross-presentation by DCs following uptake.

Further investigation aimed at dissecting the mechanisms by which QKI/PPARδ complex enhances antigen uptake will contribute to our current understanding of DC biology and may provide new strategies to improve DC-based immunotherapy.

Table of Contents

List of Illustrations

Chapter 1: Introduction

1.1 Quaking

Quaking (QKI) is an RNA-binding protein, belonging to the signal transduction and activation of RNA (STAR) protein family. It is encoded by the gene *qk* and has three main isoforms (QKI5, QKI6, and QKI-7), generated by alternative splicing (Kondo et al., 1999). As an RNA-binding protein, QKI is shown to affect translation, stability, export, splicing of mRNA and microRNA biogenesis (Darbelli & Richard, 2016). The physiological role of QKI has been mainly studied in the neural system. Ablation of expression of QKI in mice impairs the formation of neural tubes and is embryonic lethal (Noveroske et al., 2002). While the crucial role of QKI in oligodendrocytes to maintain myelination has been established for decades (Hardy, 1998), the detailed mechanism was only revealed recently (Zhou et al., 2020). Dysregulation of QKI causes various neurological diseases. In ataxia and schizophrenia patients, the expression level of QKI is significantly decreased in CNS (Åberg et al., 2006). Furthermore, chromosome 6q25-6q26 deletion, where *qk* is located, is found in 30% of glioblastoma cases (Yin et al., 2009) indicating the tumor suppressing potential of QKI.

Using $Pten^{-/-}$; $Trp53^{-/-}$ mouse model, which develops premalignant neural stem cells (NSCs), Shingu et al have demonstrated the functional significance of QKI deletion in gliomagenesis. Studies in this model showed that NSC specific deletion of qk causes downregulation crucial genes involved in phagosome formation, clathrin-mediated endocytosis, and endolysosome formation. This causes impairment of receptor recycling and endolysosome-mediated protein degradation and subsequently results in the sustained expression of proteins involved in self-renewal. This enables

glioma stem cells to maintain stemness even outside the niches and permits their hyperproliferation during invasion and migration (Shingu et al., 2017).

Another study investigating the effect of QKI on mature myelin proposed a novel mechanism where QKI function is independent of its RNA binding capacity (Zhou et al., 2020). Instead, QKI-5 interacts with the PPARδ-RXRα nuclear receptor complex as a co-activator, enhancing the expression of genes involved in lipid metabolism, particularly fatty acid elongation and desaturation. When QKI is depleted in mouse oligodendrocytes, which is essential for myelin production, the lipid component in myelin is drastically decreased and results in demyelination-associated disease phenotypes.

Recently, attention have been brought to the role of QKI in immune cells, particularly monocytes and macrophages. De Bruin et.al showed that QKI is highly expressed in atherosclerotic macrophages and reduction in QKI protein levels impaired differentiation of monocytes to macrophage along with a decrease in the uptake of lipoproteins by macrophages. The findings were also corroborated in study comparing a unique QKI-haploinsufficient atherosclerosis patient with a healthy sibling with intact copies of QKI (De Bruin et al., 2016).

Another study uncovered the anti-inflammatory role of QKI-5 in macrophages. It was shown that silencing of QKI-5 in macrophage induces the M1-like polarization, that is characterized by an increase in TNF-α and IL-6 production and a decrease in IL-10 secretion (L. Wang et al., 2017). Mechanistically, it was found that QKI-5 binds and represses NF-κB thereby limiting the STAT1-NF-κB pathway. In mouse model,

macrophage-specific depletion of QKI renders them sensitive to endotoxin challenge while overexpression of QKI-5 protected the animals against LPS-induced endotoxin shock.

Although novel functions of QKI in monocytes and macrophages have been discovered, our understanding of QKI under both physiological and disease conditions is still incomplete. Further, besides macrophages, DCs also arise after the differentiation of monocytes in response to different stimulus. These monocyte-derived dendritic cells play an important role in bridging the innate and adaptive immunity under inflammation conditions and are of great therapeutic importance. The contribution of QKI to the DC biology and to the large myeloid cell population still awaits elucidation.

1.2 PPARδ

Peroxisome proliferator-activated receptor (PPAR) δ, belongs to PPAR nuclear receptor family that consists of PPARα, PPARγ, and PPARβ/δ. Members of this receptor family largely differ in their tissue distributions, ligand specificities, and functions. While PPARα is preferentially expressed in liver, kidney and muscles, and PPARγ is mainly found in adipose tissue and macrophage, PPARδ is relatively ubiquitously expressed cross various cell types and is the least understood one among the three (Biologie & Cellulaire, 1996).

The crystal structure of PPARδ has been resolved (Zoete et al., 2007) and similar to the other two PPARs, it consists of a ligand binding domain (LBD), a DNA binding domain, a hinge and two activation function (AF) motifs. The LBD binds to a wide variety of ligands, which includes but is not limited to polyunsaturated lipid, lipoproteins, and their derivatives. Additionally, synthetic ligands such as GW501516, have been developed with high specificity and effectivity with therapeutic potential for metabolic diseases. Moreover, the LBD also induces the formation of a heterodimer with another nuclear receptor, RXR family receptor. This PPAR/RXR interaction is common to all three PPARs and is essential for their functions, which is to modulate their targeting genes by binding to PPAR response elements located in the promoter regions (Nolte et al., 1998). However, there is also evidence suggesting that PPARδ could specifically interact with β-catenin (Scholtysek et al., 2013), or NF-κB instead of RXR to regulate a different set of genes (Adhikary et al., 2015). In addition to their heterodimer partners, PPARs also interact with co-factors, either co-activators or co-suppressors, adding another layer of the complexity. The recruitment of co-factors

depends on the type of ligand, agonist or antagonist, that induces different conformational changes in the LBD and the AF-2 motif, resulting in distinct functions. QKI-5 has been found to be one of the co-activators that form a protein complex with PPARδ and RXRα to regulate a large set of gene expression in neural stem cells, oligodendrocytes and microglia, as mentioned previously (Zhou et al., 2020).

PPARδ is the least characterized protein among PPARs. Functional significance of PPARδ has been mostly focused on fatty acid metabolism and glucose homeostasis and knocking out *ppard* in mice predisposes the development of high fat induced obesity (Y. X. Wang et al., 2003). Moreover, treatment with a PPARδ agonist enhances insulin secretion and promotes fatty acid oxidation, thereby decreasing body fat in mouse. There is also evidence suggesting that PPARδ enhances mitochondrial function by promoting expression of genes involved in mitochondria respiration (Ravnskjaer et al., 2010).

The physiological role of PPARδ inflammation has been studied, though with contradicting findings. Some studies such as those conducted in EAE mouse model revealed its anti-inflammatory role in autoimmune diseases. The PPARδ agonist treatment could reduce production of pro-inflammatory cytokines TNFα and MCP-1 and reduce the disease severity (Dunn et al., 2010). On the contrary, other studies have indicated the pro-inflammatory functions of PPARδ. In psoriatic skin condition, PPARδ is found to be significantly elevated and induces TNFα secretion (Romanowska et al., 2010). Moreover, in monocyte-derived macrophages, PPARδ can bind to NF-κB and STAT1 and consequently represses their activation of downstream pro-inflammatory genes (Adhikary et al., 2015). It is also been shown that deletion of

PPARδ in macrophages decreases their phagocytic capacity, thereby limiting their T cell activation function (Mukundan et al., 2009). The role of PPARδ in inflammation, especially in immune cells, still remains inconclusive.

1.3 Dendritic Cells

Dendritic cells (DCs) are first described by Steinman and Cohn (Steinman & Cohn, 1973). They are named after the dendrite-like membrane protrusions. Their crucial roles in bridging the innate immunity to adaptive immunity was established in later studies.

DCs constantly survey the environment, detect pathogens, and relay the threat to T cells. They express a wide range of pattern recognition receptors (PRRs). PRRs can be activated by pathogen-associated molecular patterns (PAMPs) and danger-associated molecular patterns (DAMPs) that are often found in bacteria, parasites, or virus-infected cells. Once DCs get activated by pathogens via PRRs, they present the antigens to the T cell through Major Histocompatibility Complex (MHC) molecules. Extracellular antigens are internalized, processed into antigenic peptides and loaded onto MHC class II molecules for $CD4^+$ T cell activation. In contrast, the intracellular antigens are processed and loaded onto MHC class I molecules to specifically bind TCRs on $CD8^+$ T cell. In the cases when DCs are not infected by pathogens, they are still able to present extracellular antigens to CD8+ T cells through cross-presentation, a process that is unique to professional antigen presenting cells (APCs). DCs are not the only APCs capable of cross-presentation. Macrophages, B cells, and even a subset of endothelial cells under certain circumstances can cross-present and activate $CD8^+$ T cells. Yet, DCs facilitate the T cell activation by not only being able to effectively present peptide-bound MHC, but also express co-stimulatory molecules and cytokines for strong T cell activation (Wculek et al., 2020).

DCs at a resting state constantly sample and internalize the surrounding environment for evaluation of any potential threat even though no PRRs are activated. DCs at this state are considered immature (iDCs). Upon PRR stimulation, iDCs quickly upregulate MHC class I and class II expressions, load antigenic peptides on MHC molecules and prepare for antigen presentation to T cells. At the same time, co-stimulatory molecules such as 4-1BBL and OX40L are also increased to provide second stimulatory signal for T cells. In addition, depending upon the type of stimulus, DCs also secret cytokines, such as IL-4, to modulate naïve T cell differentiation. DCs at this stage are called mature DCs (mDCs).

DCs represent heterogenous populations with different ontogeny and physiological roles. They are classified into conventional DCs (cDCs), plasmacytoid DCs (pDCs), and inflammatory DCs. cDCs and pDCs are derived from precursor cells in the bone marrow whereas inflammatory DCs are differentiated from circulating monocytes under inflammation.

Among different types of DC, cDCs are the major population present at steady state. It consists of cDC1 and cDC2 and they are associated with presenting antigens to CD8+ and CD4+ T cells, respectively. Their critical role in the induction of protective immunity against bacterial and viral infection as well as different types of tumors has been extensively studied (Wculek et al., 2020). In contrast, pDCs are known for their inability to cross-present antigens at steady state. pDCs are specialized in type I interferon production in response to viral infection. Inflammatory DCs can be found at the site of injury or infection *in vivo*. They express high levels of co-stimulatory molecules such as CD80, CD86, as well as MHC molecules. In addition, human CD14+

monocytes could be differentiated to DCs *ex vivo*. These monocyte derived DCs (moDCs) exhibit similar transcription profile as *in vivo* inflammatory DCs, making them a good model to study DC biology. In fact, moDCs are widely used in cancer immunotherapy as DC vaccines alone or for the *ex vivo* generation of antigen-specific T cells with their anti-tumor effect proven by several clinical trials (Wculek et al., 2020).

1.4 Antigen uptake by dendritic cells

Dendritic cells are considered the most effective antigen presenting cells due to their superior ability to stimulate antigen-specific T cell responses. As APC, one of their key functions is to constantly sample the external environment and internalize the particles outside the cells, ranging from pathogens to apoptotic cells. The route of antigen uptake by DCs can be broadly categorized into clathrin-mediated endocytosis, phagocytosis, and micropinocytosis.

1.4.1 Clathrin-mediated endocytosis

Clathrin-mediated endocytosis is the most extensively studied mode of endocytosis, although detailed molecular mechanism studies have not been conducted with DCs. This mechanism has been shown to be highly conserved across species and different cell types (McMahon & Boucrot, 2011). The process is initiated when a membrane invagination is formed, preferentially at the PtdIns(4,5)P_2-rich membrane region. Upon endocytic receptor activation, a key adaptor protein, AP2 is recruited to the membrane curvature and binds to both PIP2 and receptor bound cargo (Höning et al., 2005). Clathrin is subsequently recruited to the cargo by AP2 and other adaptor proteins followed by quick polymerization into a clathrin-coat that wraps the outer edge of the invagination, thereby stabilizing it. As the coated pit extends to its maximal size, it internalizes sufficient particles and deforms from the plasma membrane. At this stage another protein dynamin is recruited to the neck of the vesicle and induces vesicle budding (Kosaka & Ikeda, 1983). When a clathrin-coated vesicle is cleaved off from the plasma membrane and fully internalized, HSC70 and Auxilin will dissemble the clathrin coat, releasing clathrin back to the cytosol and ready for next round of

endocytosis (Massol et al., 2006). Together, a freshly formed endosome is released for further trafficking and processing.

Clathrin-mediated endocytosis is responsible for internalizing a great variety of small molecule such as antibodies, lipoproteins and immune-complexes for presentation. The functional significance of endocytosis is not limited to antigen uptake. Chemokine and cytokine receptors such as CCR5 and IL4 that are highly expressed in DCs, are able to induce clathrin-mediated endocytosis to activate perspective signaling pathways and to recycle the receptors (McMahon & Boucrot, 2011).

1.4.2 Phagocytosis

In contrast to clathrin-dependent endocytosis, phagocytosis is dependent on remodeling of actin cytoskeleton (Freeman & Grinstein, 2014). It is worth noting that DC, as well as other professional phagocytes, such as macrophages, constantly exhibit filopodia and membrane ruffles, allowing their maximal encounter with the environment (Patel & Harrison, 2008). These membrane protrusions are formed by the cortical F-actin. Phagocytosis is initiated upon the engagement of a phagocytic receptor with targeted particles, leading to the disruption of the steady state actin cytoskeleton at the cortical membrane. When F-actin is debranched and nucleated, the lateral mobility of other phagocytosis receptors significantly increases, leading to an amplified signal for phagocytosis (Jaumouillé et al., 2014). Next, the F-actin monomers polymerize and form pseudopodia to internalize the particle. This step involves Cdc42, Rho- and Rap-family GTPases that regulate a large number of actin nucleation and polymerization proteins such as Arp2/3, coronins, and cofilins, as well

as some lipid mediators for protein anchoring (Rohatgi et al., 1999) (Yan et al., 2005) (Cai et al., 2007). However, largely due to the complexity of various upstream signals from different phagocytosis receptors the detailed molecular mechanisms regulating this step are still not completely elucidated. Finally, when the pseudopodia are extended to the maximal size and sealed the phagocytosis cup is terminated. At this point actin filaments are depolymerized and removed from the nascent phagosome (Marion et al., 2012).

Although formation of a phagosome requires consistent remodeling of the cortical cytoskeleton, the initiation driving force and the phagocytosis receptors can vary widely. Receptors that induce phagocytosis can be broadly classified into Fc receptors, scavenger receptors and integrins, which are all highly expressed in DCs (Freeman & Grinstein, 2014). Fc receptors bind to Fc portion of different classes of immunoglobulin, thereby recognizing opsonized particles. With their structural diversity, scavenger receptors can recognize a wide range of targets. For example, CD36 binds to oxidized lipids, commonly found on apoptotic cells (Jaqaman et al., 2011). Integrins, on the other hands, can be stimulated by not only specific targets (both opsonized and non-opsonized), but also by the increase in cellular rigidity (Abram & Lowell, 2009). Bacterial cells are thousand times more rigid than normal human cells or apoptotic corpses (Tuson et al., 2012). This mechano-signal can be sensed by integrins to distinguish between self and non-self-cells.

Multiple types of phagocytosis receptors can be co-expressed on a single DC. While each receptor has distinct selectivity, yet they can overlap extensively. These receptors collaborate to recognize a wide range of particles. One of the advantages of

this receptor interaction is that enables targeting of several regions recognized by different receptors on any particular particle (Uribe-Quero & Rosales, 2017). Simultaneous engagement of several receptors enables DCs to detect particles present at low concentrations in the environment and enhances the sensitivity of these particles for phagocytosis.

1.4.3 Macropinocytosis

Apart from clathrin-mediated endocytosis and phagocytosis, DCs also exhibit constant engulfment of extracellular milieu in a non-specific manner. This process is known as macropinocytosis (Liu & Roche, 2015) (Canton, 2018). Early studies have suggested that DCs as well as macrophages actively perform macropinocytosis in a relatively large volume and an entire cell can be internalized within an hour. The extensive energy spent on macropinocytosis alludes to its functional significance. However, compared to other forms of cellular engulfment, macropinocytosis still remains a less studied and underappreciated form.

Unlike endocytosis and phagocytosis which require receptors to recognize specific molecules on foreign particles or abnormal cells, macropinocytosis is initiated from the membrane ruffles that are induced by a calcium sensing GPCR, CaSR, in response to extracellular calcium, which is often elevated at the site of injury or infection (Canton et al., 2016). Due to its non-selectivity, a foreign antigen can only be internalized only when it is present in high concentrations. However, similar to phagocytosis, macropinocytosis also requires actin remodeling and is regulated by similar aforementioned actin remodeling machinery (Redka et al., 2018).

One of the reasons that macropinocytosis is less understood is that it is challenging to target it specifically. For example, inhibitors that prevent actin polymerization will simultaneously affect phagocytosis and micropinocytosis making it challenging to distinguish the two phenomena. Using different sized fluid tracer or dextran also fails to differentiate macropinocytosis from endocytosis due to the overlap of particle sizes that they are able to recognize. Some studies employed tagged-OVA to evaluate macropinocytosis in DCs. However, later it was shown that tagged-OVA can indeed be recognized by mannose receptor to induce phagocytosis (Autenrieth & Autenrieth, 2009). Therefore, further studies to differentiate these modes of cellular engulfment requires development of highly specific and efficient inhibitors or genetically knockout models.

1.5 Antigen processing and presentation

After being internalized, antigens need to be processed to peptides before being loaded to the MHC molecules. The size of antigenic peptides is restricted by the binding groove of MHC molecules. For MHC class I, this length is restricted to 8 to 11 amino acids while the number of amino acids in the peptide chain ranges from 14 to 18 for MHC class II molecules.

In classical MHC class I presentation, where endogenous antigens are presented to $CD8^+$ T cells, antigenic peptides are generated by cytosolic proteasome and subsequently recruited to the endoplasmic reticulum (ER) lumen by transporter associated with antigen processing (TAP) (Halenius et al., 2015). In the ER lumen, TAP forms a peptide-loading complex (PLC) with ERp57, tapasin, calnexin, calreticulin, and ER aminopeptidase (ERAP) (Wearsch & Cresswell, 2007). PLC is responsible for the final trimming and loading of peptides on MHC class I molecules within the ER lumen (Peaper et al., 2005). Following the loading of the peptide, the peptide-MHC complex (pMHC) is transported to the cell membrane for T cell activation.

Loading of exogenous peptides to the MHC class II molecules occurs in a specialized endosomal compartment called MHC class II compartment (MIIC) (Roche & Furuta, 2015). Pathogens are internalized and temporarily stored in either endosome or phagosome (depending on the mode of antigen uptake), which fuses with early endosome and then MIIC (Neefjes, 1999). The MIIC is highly acidic and contains various lysosomal proteases that can degrade exogenous pathogens. In addition, the newly synthesized or recycled MHC class II molecules are also delivered from ER or early endosomes to the MIIC, respectively (Griffin et al., 1997). Before reaching the

MIIC, MHC class II molecules are associated with the invariant chain (Ii) protein that prevents suboptimal loading of random peptides during trafficking. Once inside the MIIC, Ii is replaced by Class II-associated Invariant chain Peptide (CLIP). CLIP is not removed until the peptide with highest affinity to MHC class II molecules is selected. Lastly, the pMHC complex is delivered to the plasma membrane. This trafficking along the endocytic pathway is guided by Rab family GTPases. Rab5 marks the newly formed endosomes and early endosomes, which is exchanged for Rab7 that marks the late endosomes (Bertram et al., 2002). Depletion of either one impairs the fusion of endosome with MIIC, thereby reducing MHC class II presentation (Egami et al., 2014).

The mechanism for presentation of endogenous antigens has been extensively studied and characterized. Yet there is limited understanding of cross-presentation of exogenous antigens to MHC class I molecules. To explain this phenomenon, two major pathways have been proposed and widely accepted, namely cytosolic and vacuolar pathways. However, to what extent these two pathways contribute to the overall cross-presentation is still debatable and difficult to quantify. Currently most evidence points to the cytosolic pathway (Schuette & Burgdorf, 2014).

In the vacuolar pathway, the internalized antigens remain in the endosomal compartments all the time (Joffre et al., 2012). Starting from early endosome or phagosome, the fusion with late endosome to exposure of antigens to proteases in the lysosome that degrade antigens to antigenic peptides and subsequent loading of the peptides to the MHC class I molecules. However, the highly acidic environment in the endolysosome is not optimal for antigen loading (Delamarre et al., 2005). Antigenic

peptides may be trimmed into individual amino acids before being loaded to MHC class I molecules, thereby limiting the cross-presentation. DCs, as potent APCs, have evolved mechanisms to overcome these limitations. NADPH oxidase 2 (NOX2) consumes proton for ROS production and can thus slow down the acidification process. NOX2 is specially recruited to the endosomal compartments in the DCs with help from Rab27a and Rac1 (Savina et al., 2006). In addition, V-ATPase is expressed to a lower level in DCs compared to other phagocytes, which further reduces the level of protons present in the endosomal compartment and enhances the availability of peptides for cross-presentation (Savina et al., 2006). Cross-presentation utilizing this pathway is sensitive to lysosomal protease inhibitors, such as cathepsin S inhibitor, whereas the cytosolic pathway is sensitive to proteasome inhibitors, suggesting the involvement of cytosolic proteases in the processing of antigens for cross-presentation.

The cytosolic pathway requires antigens to be transported from early endosome or phagosome to the cytosol. How antigens, which may be large in size, get actively transported across endosomal membranes still remains unanswered. Although accumulating evidence suggests the involvement of ER associated degradation (ERAD) machinery in this process (Ackerman et al., 2006), some studies also support the idea that endocytic membrane disruption leads to antigen leakage (Dingjan et al., 2016). The antigen degradation following transportation to the cytosol is found to hijack the mechanism that is utilized by the classical MHC class I presentation. Specifically, TAP and ERAP are shown to be responsible for antigen degradation for cross-presentation. They are found in the endosomes containing peptide-loaded MHC for final transport to the plasma membrane. However, this does not exclude the possibility that these proteins are recruited to the antigen-containing endosomes before antigen

digestion, in which case it is not necessary for antigens to be exported outside endosomes for degradation.

Nevertheless, the crucial role of the Rab family GTPases is not questionable. They are involved in sorting, trafficking, and processing of various endosomal compartment. A study screening 52 Rab proteins in a murine DC-like cell line revealed that 12 of them are essential for antigen cross-presentation (Zou et al., 2009). The functional significances of some of them have been reported. For example, Rab27a contributes to the incorporation of NOX2 to the endosomes (Jancic et al., 2007). Rab11 recruits the MHC class I molecules to the antigen-containing phagosomes (Ullrich et al., 1996). Rab34 guides the fusion of phagolysosomes (Egami et al., 2014).

Our current understanding of antigen cross-presentation in DCs remains incomplete and the proposed models cannot be fully supported by existing evidence. Moreover, many of these studies are conducted in murine system. Whether these findings in mouse can be validated in human cells is still unclear and warrants further research in this area.

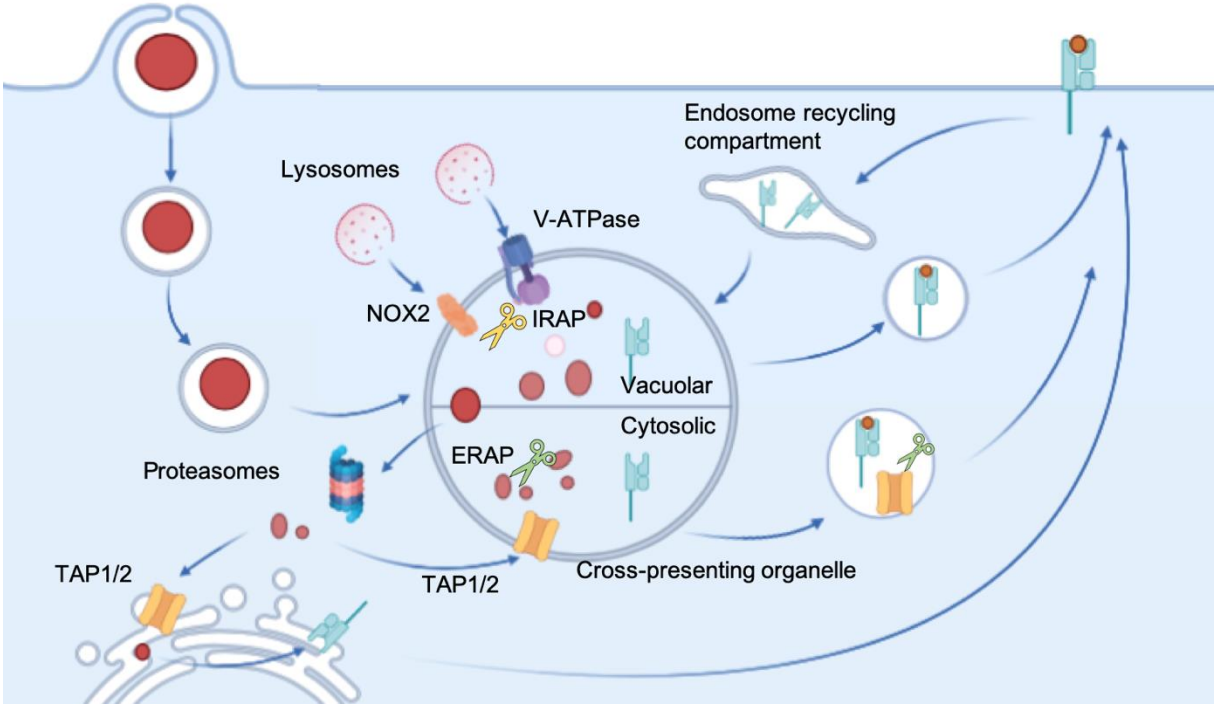

Figure 1: Intracellular pathways for cross-presentation in dendritic cells.

After being taken up, exogenous antigens are processed in two different pathways. In the vacuolar pathway, the antigens are degraded and processed in the endosomes/phagosomes by fusing with protease-containing lysosomes and MHC Class I-containing recycling endosomes. The exogenous antigens can also be exported to the cytosol and degraded by cytosolic proteasomes. Processed antigens are transported into ER for MHC Class I loading. Alternatively, they can be transported back to endosomes/phagosomes for MHC Class I loading and surface presenting. TAP, transporter associated with antigen processing; NOX2, NADPH oxidase 2; ERAP, ER-associated aminopeptidase; IRAP, insulin-responsive aminopeptidase.

Chapter 2: Materials and Methods

2.1 Generation of human monocyte derived DCs

$CD14^{+}CD16^{-}$ monocytes were isolated from previously frozen leukapheresis products from healthy donors using EasySep™ human monocyte isolation kit according to manufacturer's instructions (STEMCELL Technologies). Cells were cultured in 6-well plates at 0.67×10^{6}cells/ml in 3 ml of AIM-V containing 800IU/ml of GM-CSF and 500 IU/ml of IL-4 for 7 days as previously described (ref). Mature DCs were stimulated with 100 ng/ml of LPS for 24 hours before being harvested.

2.2 Isolation of Peripheral Mononucleocytes (PMN)

PMNs were isolated from a buffy coat obtained from MD Anderson Blood Bank using the gradient centrifugation method. Briefly, in a 50 ml canonical tube, 20 ml of diluted blood was layered on top of 10 ml of Histopaque-1077 (Sigma-Aldrich) and 10 ml of Histopaque-1119 (Sigma-Aldrich). After centrifugation for 30 minutes at 2000 rpm, the layer between Histopaque-1077 and Histopaque-1119, which contained PMNs, was collected. PMNs were washed with RPMI-1640 (Gibco) and counted before subjecting them to three rounds of freeze/thaw for cell lysis.

2.3 Generation of M27 CTLs

The MART-1 specific cytotoxic T cell lymphocytes (M27 CTLs) was generated as previously described (Park et al., 2017). Briefly, PBMCs isolated from leukapheresis products were cultured in AIM-V media containing 800 IU/ml of GM-CSF and 500 IU/ml of IL-4 for 7 days for generation of DCs. DCs were matured using 2 ng/ml of IL-1β, 1000 IU/ml of IL-6, 10 ng/ml of TNFα and 1 μg/ml of prostaglandin E2 for at least 18

hours. Matured DCs were harvested and pulsed with 40 μg/ml of M27 peptide (PolyPeptide Group) and 3 μg/ml of β2-microglobulin (Scripps Laboratories) in PBS containing 1% of human serum albumin (Life Technology) for 4 hours at room temperature before they were washed and irradiated. Peptide pulsed DCs were subsequently used to co-culture with PBMCs at ratio of 1:10 in presence of IL21 and low does IL-2. The DC stimulation took two rounds and each round took 7 days. M27-tetramer^{+} CD8^{+} cells were sorted at the end of DC stimulation and expanded using the rapid expansion protocol (Park et al., 2017).

2.4 Co-immunoprecipitation

Cells were cross-linked in 1% formaldehyde for 10 minutes at 37°C and then neutralized by Glycine before harvested. Cells were subsequently incubated in 0.3% NP-40 lysis buffer supplemented with proteinase inhibitor at 4°C for 30 minutes and centrifuged for 30 minutes. Cell lysate was sonicated using a Dounce biohomogenizer. Protein concentrations were quantified using Bradford Assay (BioRad) as manufacturer instructed. Isolated proteins were incubated with indicated antibodies overnight at 4°C before Dynabeads^{TM} protein G for immunoprecipitation (ThermoFisher) was added to the mixture to pull down the QKI-5/PPARδ complex. The immunoprecipitation products were subjected for immunoblotting.

2.5 Immunoblotting

Cells were harvested, washed with ice-cold PBS and lysed in RIPA lysis buffer (ThermoFisher). Protein concentrations were quantified using Bradford Assay (BioRad) as manufacturer instructed. 15-30 μg of protein was subjected to SDS-PAGE on a NuPAGE^{TM} polyacrylamide gel (ThermoFisher) and transferred to a nitrocellulose

membrane using the Turbo™ Trans Blot system (Bio-Rad). The membrane was blocked in 5% non-fat milk overnight 4°C and incubated with indicated primary antibodies for at least 4 hours. The membrane was then washed and incubated with HRP-conjugated secondary antibodies before visualized using SuperSignal™ chemiluminescence system (Thermo Fisher).

2.6 siRNA Knockdown

Several siRNAs targeting QKI-5 and PPARδ were obtained from Dharmacon. N-TER™ Nanoparticle siRNA transfection system was used to transfect 50 nM siRNAs to DCs according to manufacturer's instructions. Transfecting media were removed 24 hours post transfection and fresh media were replenished.

2.7 Quantitative RT-PCR

Cells were harvested and washed three times in PBS before RNA isolation. Total RNA was isolated using the RNeasy Mini Kit (Qiagen) following manufacturer's instructions. RNA concentration was determined by NanoDrop spectrophotometer (ThermoFisher Scientific). The reverse transcription reaction was performed on the same amount of RNA across different samples, using the M-MLV Reverse transcriptase (ThermoFisher Scientific) as per manufacturer's instructions. Quantitative PCR was performed in duplicates using SYBR™ Select Master Mix (Applied Biosystems) and QuantStudio 5 Real-Time PCR System (ThermoFischer Scientific) according to manufacturers' instructions. The housekeeping gene Rpl13a was used for normalization. The primers used are listed as follow: Qk forward: ATCCTATTGAACCTAGTGGTGTA, reverse: GGTCAGAAGGTCATAGGTTAGTT; Ppard forward: CTCTATCGTCAACAAGGACG, reverse:

GTCTTCTTGATCCGCTGCAT; Cpt1a forward: CAGGCCGAAAACCCATGTTG, reverse: CCACCAGTCGCTCACGTAAT; Pdk4 forward: ACAGACAGGAAACCCAAGCC, reverse: TTGCCCGCATTGCATTCTTA; Rpl13a forward: CCTCAAGGTCGTGCGTCTGA, reverse; TCCACGTTCTTCTCGGCCTG.

2.8 Phagocytosis Assay

The Phagocytosis Assay Kit (IgG FITC) (Cayman Chemical) was used to evaluate the phagocytic capacity. Cells were harvested and resuspended at a concentration of 1×10^6cells/ml. The latex beads-rabbit IgG-FITC complex was directly added to the cell suspension at a final dilution of 1:200. Cells were subsequently cultured at 37°C for indicated periods of time. Before measuring the fluorescent signal on a flow cytometer, cells were briefly resuspended in trypan blue for 5 minutes to quench the surface signal, in order to distinguish the internalized beads from surface bound beads.

2.9 Flow cytometry

All antibodies for flow cytometry were procured from Biolegend. The panel consisted of CD36-FITC (336204), CD8-APC/Cy7 (344714), Ki67-PE (1512109), IFNγ-BV650 (502538), perforin -PE/Cy7 (353316), granzyme B-APC (372204), HLA-DR-BV421 (307636), CD80-BV510 (305233), CD83-BV785 (305338), and CD86-BV650 (105035). For surface markers, cells were treated with TruStain FcX™ (Biolegend, 422301) as instructed by the manufacturer before staining with antibodies at a dilution of 1:100 for 15 minutes at room temperature. Stained cells were subsequently washed three times with ice-cold PBS supplemented with 1%FBS before acquiring data by

flow-cytometry. For intracellular staining, cells were treated with Brefeldin A (Life Technology) to block the secretion of cytokines for 18 hours. The Intracellular Fixation and Permeabilization Buffer Set (Invitrogen) was used for intracellular antibody staining according to manufacturer's instructions. Antibodies against intracellular targets were used at 1:50 dilution. All FACS data was acquired using Novocyte flow cytometer and analyzed using FlowJo software (Tree Star).

2.10 Statistics

Data analysis was performed using GraphPad Prism 8 (GraphPad Software Inc). Data were presented as mean $\pm$ s.e.m. Statistical tests were considered significant if *P*-values were < 0.05

Chapter 3: Results

3.1 Expression of QKI-5 and PPARδ in dendritic cells

First, to validate the expression of QKI-5 and PPARδ complex in human monocyte derived dendritic cells (moDCs), immunoblotting against QKI-5 was performed to detect protein levels of QKI-5 and PPARδ. Generation of moDC started with peripheral monocytes, which were cultured in medium containing GM-CSF and IL-4 for 6 days to induce their differentiation to immature DCs. Maturation of iDCs can be stimulated by various PAMPs or DAMPs, commonly used are TNFα in combination with IL-1β, or LPS alone. QKI-5 protein was not detectable in freshly isolated monocytes. However, its expression was detectable as early as 2 days after differentiation into iDCs and increased till day 4 and then remained stable till day 6, suggesting QKI-5 plays a specific role in moDCs. Mature DCs (mDCs), either TNFα induced or LPS induced, also expressed QKI-5 at a similar level to the Day 4 and Day 6 iDCs. The protein expression of PPARδ showed the same trend as QKI-5. However, RXRα, a common heterodimerization partner of PPARδ was expressed at very low levels in day 4 and day 6 iDCs and was not detectable in monocytes and mDCs (Fig 2).

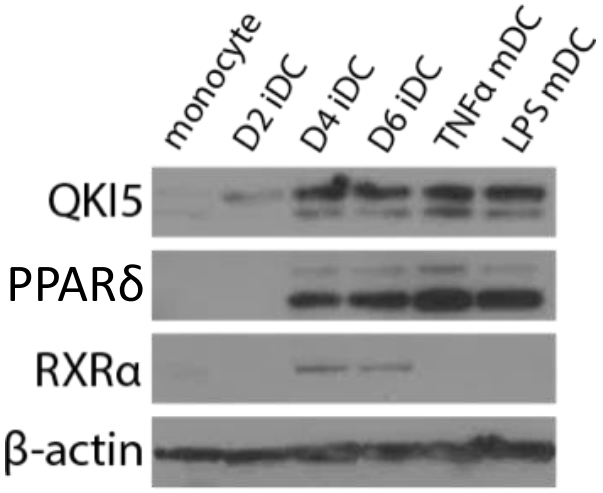

Figure 2: QKI5 and PPARδ were upregulated upon monocyte differentiation

$CD14^{+}CD16^{-}$ monocytes isolated from peripheral blood were cultured in AIM-V medium containing 800 IU/ml of GM-CSF and 500 IU/ml of IL-4 for indicated periods of time. Mature DCs were cultured for 6 days and then stimulated with either 10 ng/ml of TNFα or 100 ng/ml of LPS for an additional 24 hours. Cells were lysed using RIPA lysis buffer supplemented with protease inhibitor. Protein levels were measured by immunoblotting. D2, day 2; D4, day 4; D6, day6; iDC, immature DC; mDC, mature DC.

Next the association of QKI-5 is with PPARδ in the moDCs was determined. PPAPδ was immunoprecipitated from iDCs. QKI-5 antibody and IgG were used as positive and negative controls, respectively. QKI-5 was detected in the QKI-5- and PPARδ- but not rabbit IgG-immunoprecipitated aggregates, indicating the association of QKI-5 and PPARδ in moDCs (Fig 3). Together, these data suggested a potential distinct function of QKI-5/PPARδ complex in moDCs that is absent in monocytes.

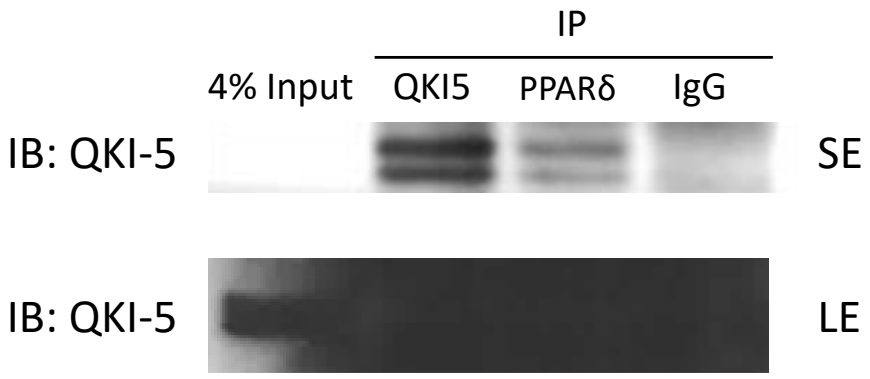

Figure 3: QKI5 and PPARδ were associated in iDCs.

Immature DCs were generated from $CD14^{+}CD16^{-}$ monocytes using GM-CSF and IL-4 for 6 days as previously described. Cells were cross-linked and then neutralized before protein isolation. QKI-5, PPARδ, and IgG were immunoprecipitated using protein G beads. Rabbit IgG antibody was included as negative control. The immunoprecipitated proteins were then subjected to immunoblot for QKI-5 expression. IP, immunoprecipitation; IB, immunoblotting; SE, short exposure; LE, long exposure.

3.2 Effect of PPARδ agonist on phagocytosis by dendritic cells

To investigate the role of QKI-5/PPARδ complex in antigen uptake and cross-presentation. PPARδ specific agonist, GW501516, was used to enhance the function of the QKI-5/PPARδ complex. The optimal drug treatment scheme was determined based on the surface expression of the scavenger receptor CD36, a common target of QKI-5 and PPARδ. Adding GW501516 on the day when monocytes were plated enhanced the surface expression of CD36 to the maximum. Treatment of the cells for 48 hours resulted in a very small increase in CD36 (Fig 4). In addition, GW501516 did not enhance the CD36 surface level in mDCs. This was expected since DCs are known to suppress the antigen uptake machinery when matured. It is also worth noting an increase in the concentrations of GW501516 for treatment of the cells did not lead to a further increase in the expression of CD36, suggesting it was saturated at 100nM. GW501516 also increased the mRNA expression levels of other QKI-5 and PPARδ common targets, namely *Cpt1a* and *Pdk4*, in iDCs generated from three healthy donors (Fig 5), suggesting GW501516 is able to enhance the function of QKI-5/PPARδ complex.

To test if enhancing the function of QKI-5/PPARδ complex affects the differentiation of moDCs, CD14 and CD209 expressions were assessed by flow cytometry. Monocytes express high levels of CD14, which is significantly reduced upon differentiation to moDCs. CD209 is a moDC-specific marker and is drastically upregulated in response to IL-4 during moDC differentiation (Sander et al., 2017). When monocytes were cultured in presence of GM-CSF and IL-4, CD14 expression were reduced to the same levels in different concentrations of GW501516-treated and vehicle-treated cells. Similarly, CD209 increased to the same extent regardless of the

treatments that cells received (Fig 6). Furthermore, the differentiation efficiency (i.e. number of moDCs harvested/the number of monocytes plated) did not differ between GW501516-treated or untreated cells. In sum, PPARδ agonist does not the affect the the differentiation process of moDCs.

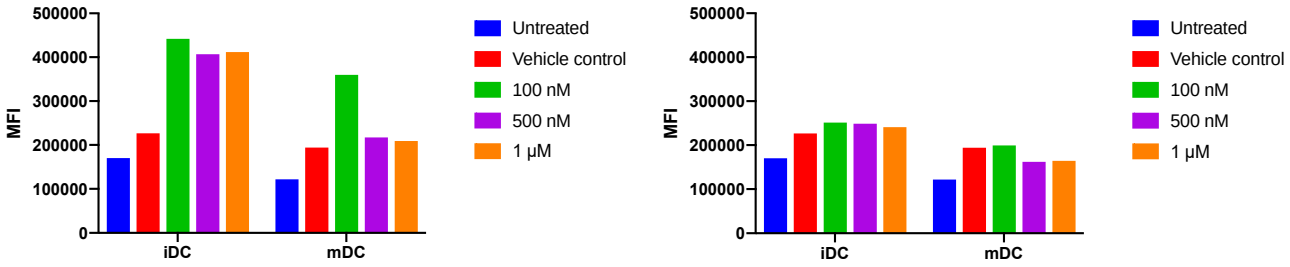

Figure 4: GW501516 enhanced CD36 expression in iDCs

Immature DCs were generated from $CD14^{+}CD16^{-}$ monocytes using GM-CSF and IL-4 for 6 days as previously described. Mature DCs were stimulated with 100 ng/ml of LPS for an additional 48 hours. iDCs or mDCs were treated with GW501516 at indicated concentrations for 7 days (top) or 2 days (bottom). Cell surface expression of CD36 was measured by flow cytometry. MFI, mean fluorescent intensity.

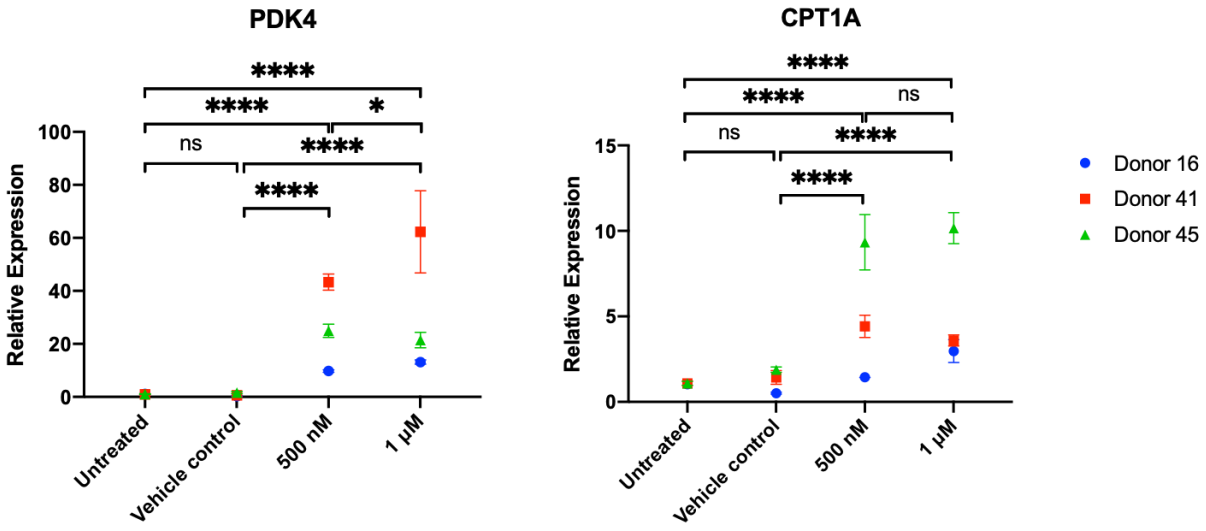

Figure 5: GW501516 upregulated QKI5 targets in iDCs

Immature DCs were generated as previously described. PPARδ agonist, GW501516 was added on day 0 of the cell culture at indicated concentrations. Expression levels of QKI-5 targeting genes, Pdk4 and Cpt1a, were analyzed via quantitative real-time PCR. Relative expression to untreated samples is plotted here. RPL13A was used a housekeeping gene for normalization. Data represent results from 3 healthy donors. n = 2. P values were calculated using two-way ANOVA and adjusted for multiple comparison using the Benjamini, Krieger and Yekutieli FDR correction; ns, not significant, *P ≤ 0.05; ****P ≤ 0.0001.

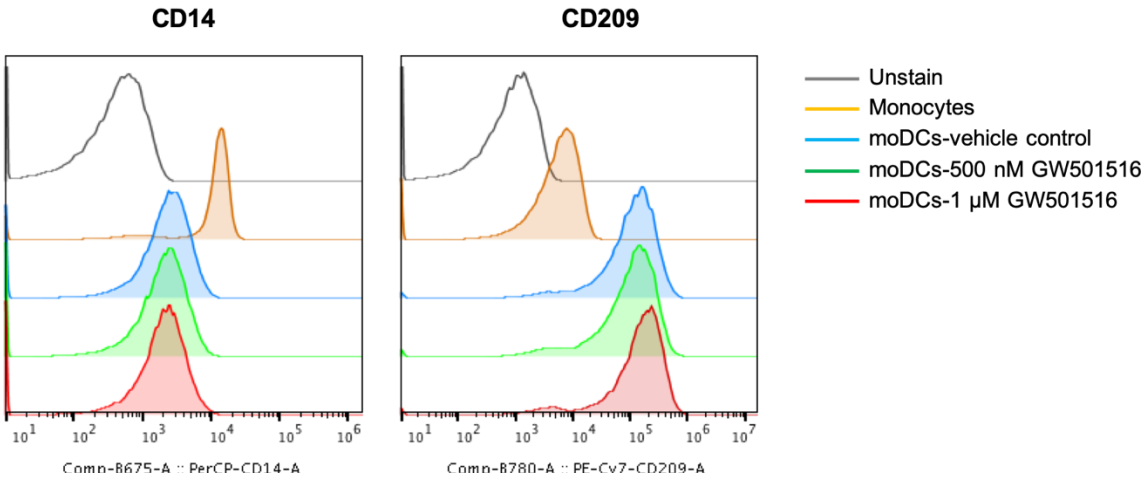

Figure 6: GW501516 did not affect the differentiation of moDCs

Monocytes were isolated from human PBMCs. Immature DCs were generated as previously described. PPARδ agonist, GW501516 was added on day 0 of the cell culture at indicated concentrations. Cell surface expression of CD14 (Left) and CD209 (Right) were measured by flow cytometry. The histogram represents three independent experiments.

Next, the effect of GW501516 on the phagocytosis by moDCs was evaluated using fluorescent labeled latex beads. When the beads were added to the DC culture, the magnitude of the fluorescent signal emitted by DCs indicated the quantity of beads that were internalized by the DCs, reflecting their phagocytic capacity. In DCs generated from three healthy donors, GW501516 increased the phagocytic capacity of iDCs to various degree at 48 hours (Fig 7). Again, mDCs were expected to exhibit low phagocytic activity. Surprisingly, GW501516 was able to enhance phagocytosis by mDCs in one donor but not the other two, suggesting that in this particular sample, the effect of GW501516 overcame the maturation induced transcriptional suppression of antigen uptake.

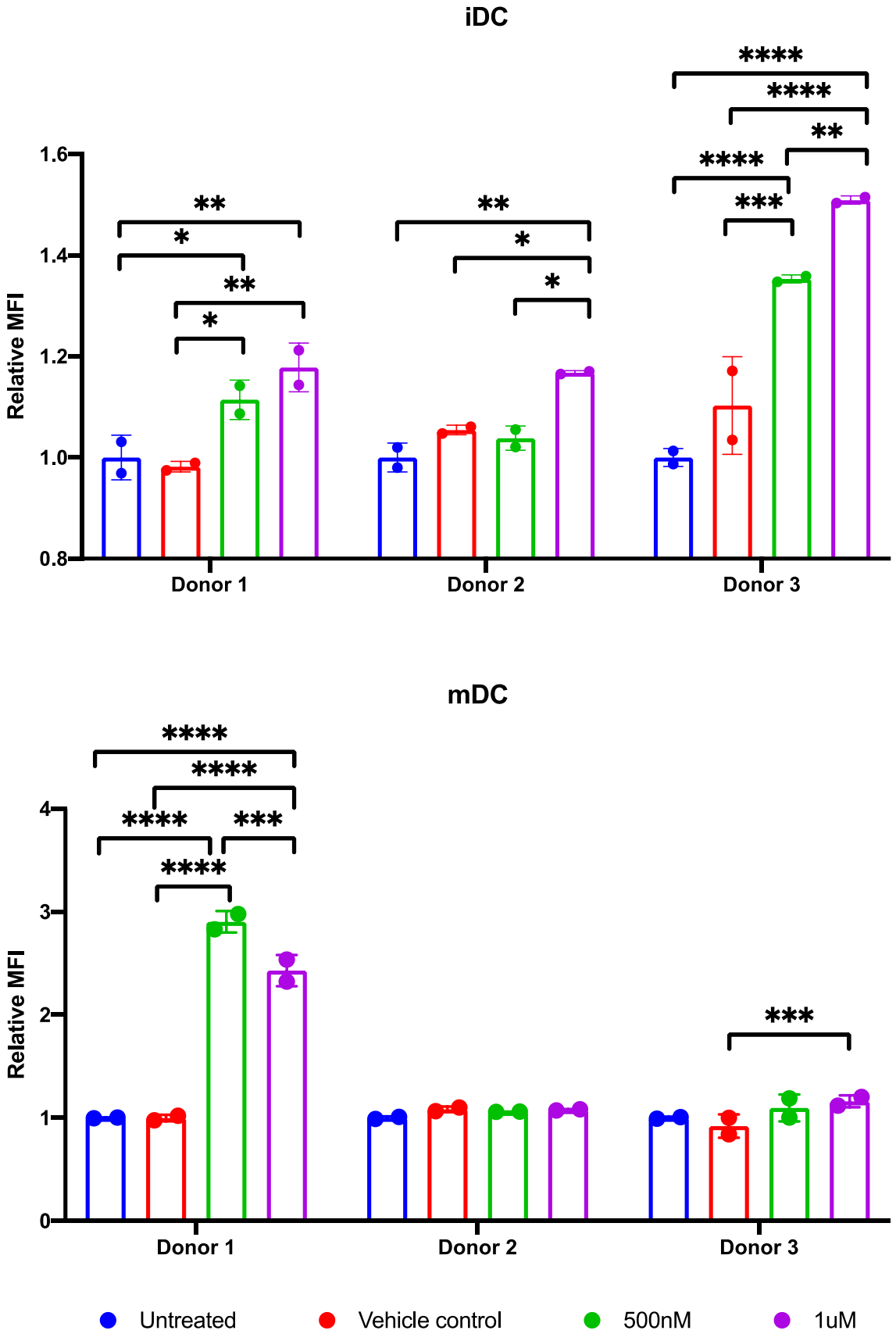
iDC
Relative MFI
1.6
1.4
1.2
1.0
0.8
Donor 1
Donor 2
Donor 3
mDC
Relative MFI
4
3
2
1
0
Donor 1
Donor 2
Donor 3
Untreated
Vehicle control
500nM
1uM

Figure 7: PPARδ agonist enhanced phagocytosis capacity of iDC

Immature DCs were generated from $CD14^{+}CD16^{-}$ monocytes using GM-CSF and IL-4 for 6 days as previously described. Mature DCs were stimulated with 100 ng/ml of LPS for an additional 24 hours. DCs were harvested and incubated with latex Beads-Rabbit IgG-FITC complex at 200:1 (v/v) ratio for 48 hours. Cells were briefly incubated with trypan blue to quench cell surface staining after incubation. The fluorescent signal emitted by internalized beads was assessed by flow cytometry. Results from three healthy donors are shown here. Data are presented as mean ± s.e.m. P values were calculated using two-way ANOVA with Turkey's multiple comparisons test. P value is not significant unless otherwise indicated. Relative MFI was calculated as MFI value of treated sample divided by untreated sample. MFI, mean fluorescent intensity; *$P \leq 0.05$, **$P \leq 0.01$, ***$P \leq 0.001$, ****$P \leq 0.0001$.

3.3 Effect of siRNA silencing QKI-5 or PPARδ on phagocytosis by dendritic cells

Ideally, GW501516 should boost the function of the QKI-5/PPARδ complex. However, it is still possible any effect that the drug may have on DCs can be attribute to PPARδ alone, especially when used at high concentration. To corroborate the role of QKI-5 in phagocytosis, individual siRNAs targeting QKI-5 or PPARδ were used to suppress their expressions in iDCs and phagocytic activity was evaluated. siRNAs targeting QKI reduced around 30% to 40% of the QKI mRNA and reduced QKI-5 protein expression to a lesser extent (Fig 8). Similarly, siRNAs targeting PPARδ reduced around 50% abundance of PPARδ mRNA and decreased the protein expression to various degrees. Interestingly, targeting PPARδ downregulated the QKI mRNA abundance but not vice versa. Moreover, targeting either QKI or PPARδ decreased the protein expressions of both to various extent (Fig 8). Nevertheless, the phagocytosis activity was decreased in iDCs to different degrees at 48 hours with siPPARδs conferring the highest suppression (Fig 9). These data strongly suggested both PPARδ and QKI-5 regulate the phagocytosis activity in iDCs.

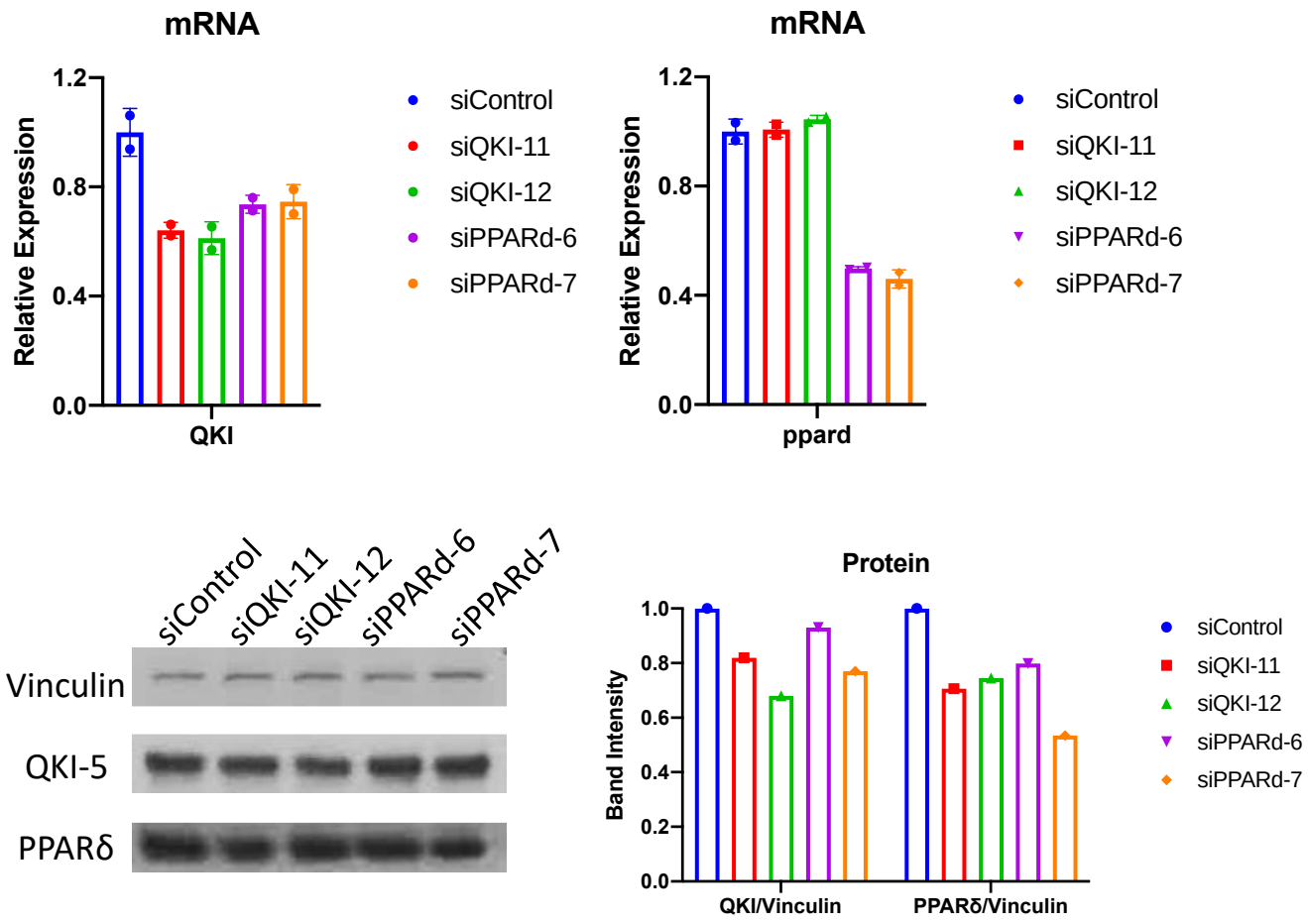

Figure 8: siRNA silencing QKI-5 or PPARδ in iDCs

Immature DCs were generated from $CD14^{+}CD16^{-}$ monocytes using GM-CSF and IL-4 for 6 days as previously described. Two different siRNAs targeting QKI-5 or PPARδ were tranfected to iDCs at concentration of 50nM using the N-TER transfection reagent on first day of iDC generation. Negative siRNA control was used to distinguish specific and non-specific targeting. Culture media containing siRNA were removed 24 hours post transfection and replenished with fresh media. Cells were harvest for quantitative RT-PCR (top) and immunoblotting (bottom) to evaluate the effect of silencing. RPL13A was used as housekeeping gene for normalization in RT-qPCR. Vinculin was immunoblotted as a loading control. Band intensity was measured by ImageJ to quantify the protein expression. siControl, siRNA negative control.

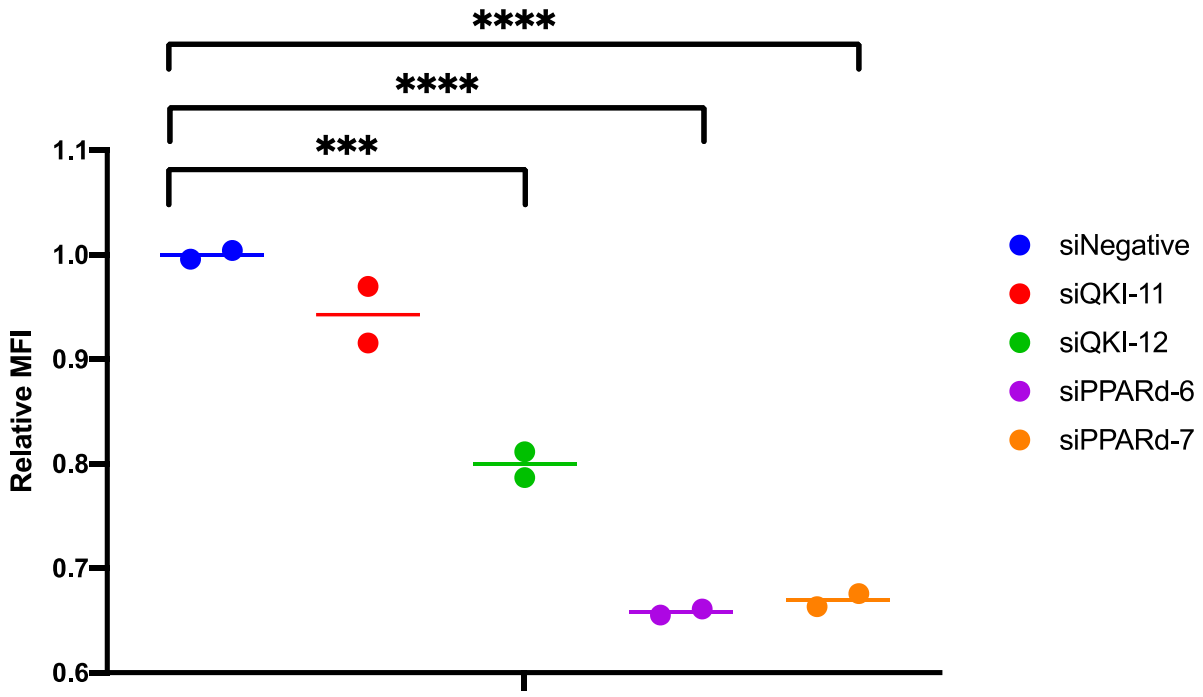

Figure 9: Knocking down QKI-5 or PPARδ impaired phagocytosis capacity of iDC.

Immature DCs were generated from $CD14^{+}CD16^{-}$ monocytes using GM-CSF and IL-4 for 6 days as previously described. Two different siRNAs targeting QKI-5 or PPARδ were tranfected to iDCs at concentration of 50nM using the N-TER transfection reagent on first day of iDC generation. Negative siRNA control was used to distinguish specific and non-specific targeting. Culture media containing siRNA were removed 24 hours post transfection and replenished with fresh media. Cells were harvested and incubated with latex Beads-Rabbit IgG-FITC complex at 200:1 (v/v) ratio for 48 hours. Cells were briefly incubated with trypan blue to quench cell surface staining after incubation. The fluorescent signal emitted by internalized beads was assessed by flow cytometry. n = 3. Data are presented as mean ± s.e.m. P values were calculated using ordinary one-way ANOVA with Dunnett's comparisons test against the control group.

Relative MFI was calculated as MFI value of treated sample divided by untreated sample. P value is not significant unless otherwise indicated. siControl, siRNA negative control; MFI, mean fluorescent intensity; ***P ≤ 0.001, ****P ≤ 0.0001.

3.4 Effect of PPARδ agonist on antigen cross-presentation by dendritic cells

To test whether the increase in phagocytic capacity by GW501516 enhances the antigen cross-presentation by DCs, several approaches were employed.

First, DCs were treated with 12.5 μg/ml of whole MART-1 protein one day before they were matured using LPS (Fig 10). Once the protein got internalized and cross-presented, these mDCs should be able to re-stimulate HLA-matched antigen-specific CTLs, i.e. M27 CTLs. M27 peptide pulsed-DCs were used as positive control while NY-ESO peptide pulsed-DCs and un-pulsed DCs were used as negative controls (Fig 10). The capacity of DC-induced T cell response was measured as T cell proliferation and effector cytokine production. M27 CTLs co-cultured with whole MART-1 protein-fedDCs were not activated as they showed no increase in IFNγ, perforin A and Ki67 stainings compared to negative controls, regardless whether they were GW501516 treated or not (Fig 11).

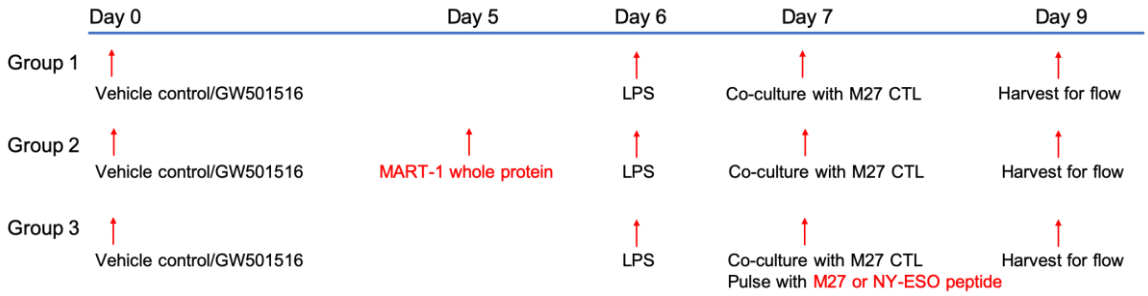

Figure 10: Experimental scheme for MART-1 whole protein cross-presentation assay

Immature DCs were generated from $CD14^{+}CD16^{-}$ monocytes using GM-CSF and IL-4 for 6 days as previously described with either GW501516 or vehicle control treatments on the first day of DC generation. On Day 5, the testing group was treated with 12.5 µg/ml of MART-1 whole protein. On Day 6, DCs were matured with LPS at concentration of 100 ng/ml before they were co-cultured with M27 CTL at 1:10 ratio. The positive control group was pulsed with 40 µg/ml of M27 peptide. Cells in negative control group were either pulsed with 40 µg/ml of NY-ESO peptide or had no antigen exposure. Two days post DC/T cell co-culture, cells were harvested for assessment using flow cytometry.

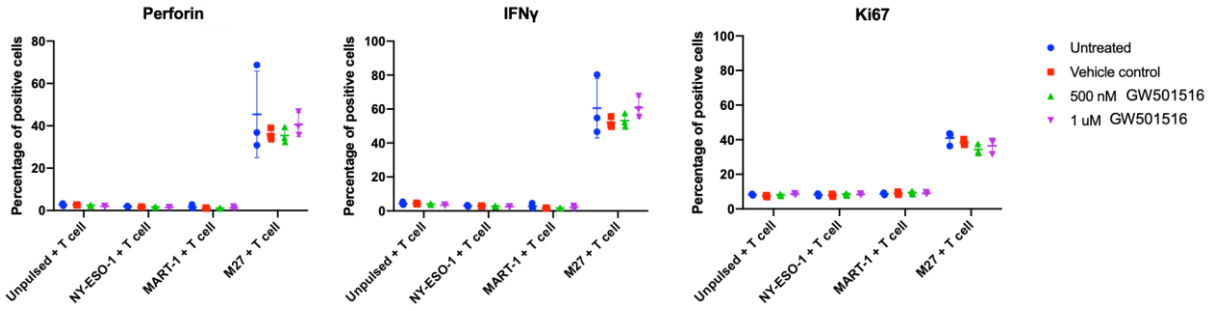

Figure 11: DCs fed with MART-1 whole protein failed to elicit M27 CTL response

M27 CTLs co-cultured with MART-1 whole protein fed DCs were harvested. Brefeldin A was used to block the cytokine secretion 18 hours before cells were harvested. Cells were washed and treated with permeabilization solution before stained with CD8-APC/Cy7, Ki67-PE, perforin-PE/Cy7, IFNγ-BV650 and Live/Dead Aqua. Stained cells were assessed by flow cytometry. The expression analysis of indicated proteins were gated on $CD8^+$ viable cells. The percentages of cells that were positive for indicated proteins are shown here. n = 3. Data are presented as mean ± s.e.m. P values were calculated using two-way ANOVA with Turkey's multiple comparisons test. P value is not significant unless otherwise indicated.

Second approach involved treatment of DCs with irradiated tumor cells with high MART-1 protein expression (A2058 cell line). The tumor cell lysate was present in the DC culture media for 2 or 5 days before DCs were matured and harvested (Fig 12). Again, these DCs were subsequently co-cultured with HLA-matched M27 CTLs. The T cell response was measured as effector cytokine production. DCs that were not fed with cell lysate were used as negative control and non-fed DCs pulsed with M27 peptides were used as positive control. In addition, M27 CTLs could be directly activated by the HLA-matched, MART-1 expressing tumor cells (Mel526), but not A2058 cells since they were HLA-mismatched (Fig 13). DCs co-cultured with MART-1 expressing tumor cell lysate failed to simulate M27 CTLs as shown by granzyme b (Fig 13, top) and IFNγ secretion (Fig 13, bottom), regardless of how long the cell lysate was present in the DC culture and regardless of whether DCs were treated with GW501516. Further investigation on these DCs revealed that their co-stimulatory molecule CD80, CD86 and CD83 are drastically decreased if they were fed with tumor cell lysate (Fig 14), which may partially explain why they were unable to induce CTL response.

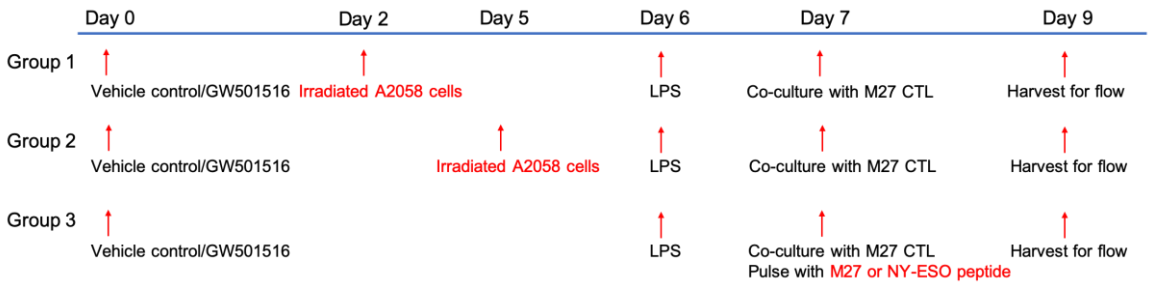

Figure 12: Experimental scheme for A2058 cell cross-presentation assay

Immature DCs were generated from $CD14^{+}CD16^{-}$ monocytes using GM-CSF and IL-4 for 6 days as previously described with either 500nM GW501516 or vehicle control treatments on the first day of DC generation. On Day 2 or 5, the testing groups were added irradiated A2058 cells at 1:10 ratio (DC:A2058). On Day 6, DCs were matured with LPS at concentration of 100 ng/ml before they were co-cultured with M27 CTL at 1:10 ratio. The positive control group was not treated with A2058 cell lysate and pulsed with 40 µg/ml of M27 peptide. Cells in negative control group were either pulsed with 40 µg/ml of NY-ESO peptide or had no antigen exposure. Two days post DC/T cell co-culture, cells were harvested for assessment using flow cytometry.

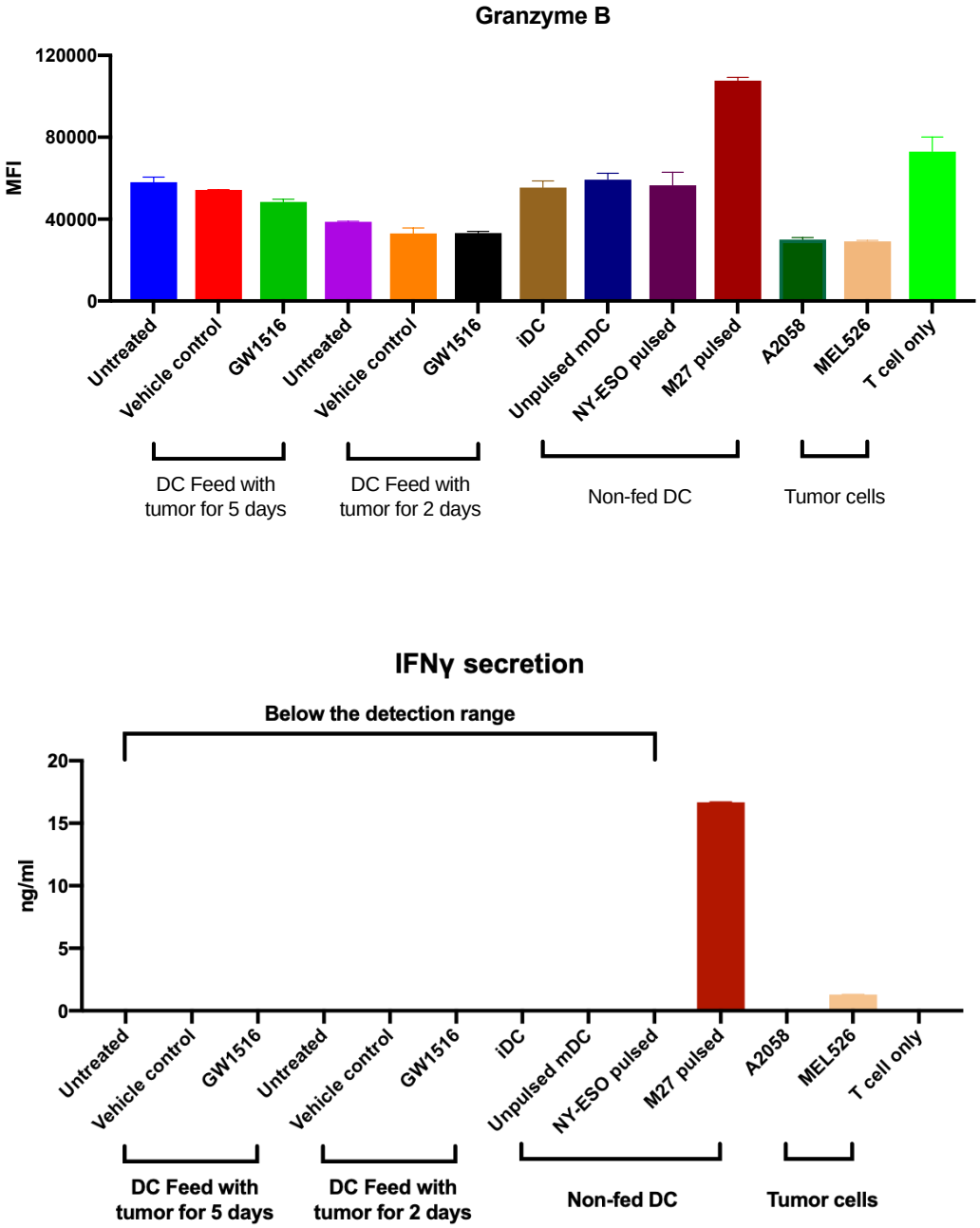

Figure 13: DCs fed with A2058 cell lysate failed to elicit M27 CTL response

M27 CTLs co-cultured with A2058 cell lysate fed DCs were harvested. Brefeldin A was used to block the cytokine secretion 18 hours before cells were harvested. Cells were washed and treated with permeabilization solution before stained with CD8-APC/Cy7,

granzyme b-APC and Live/Dead Aqua. Stained cells were assessed by flow cytometry. The expression analysis of indicated proteins were gated on $CD8^+$ viable cells. Before bredfeldin A was added, cell culture supernatants were harvested and use for ELISA analysis to detect IFNγ secretion. MFI, mean fluorescent intensity. n = 2. Data are presented as mean ± s.e.m.

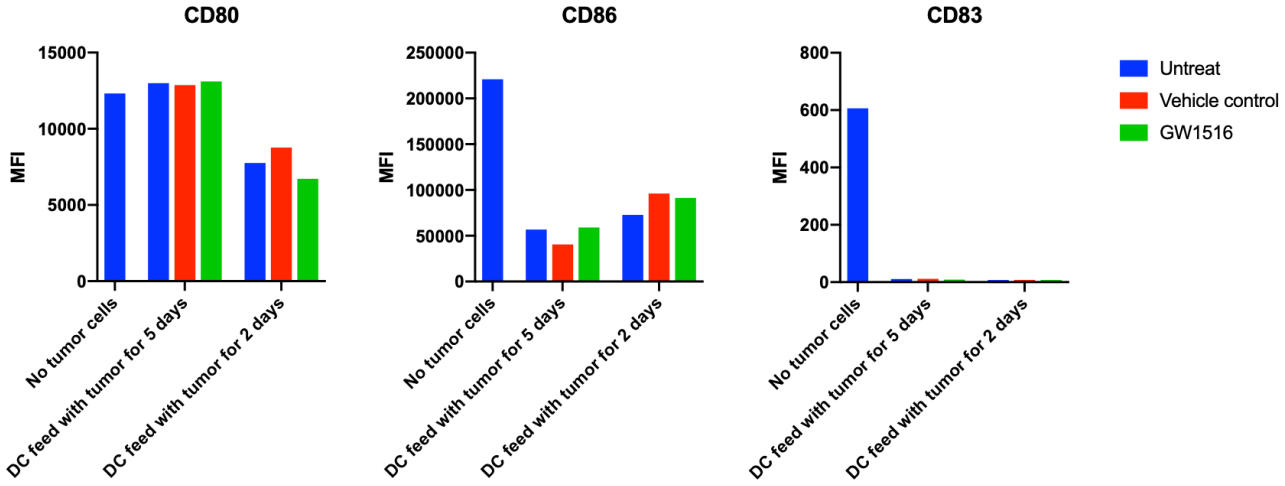

Figure 14: Expressions of co-stimulatory molecules by DCs were downregulated upon A2058 cell lysate exposure

A2058 cell lysate fed-DCs were generated as previously described. DCs were harvested for flow cytometry before M27 CTL co-culturing in order to assess the expression of co-stimulatory molecules. Cells were washed and stained with HLA-DR-BV421, CD80-BV510, CD83-BV785, and CD86-BV650 antibodies. Cells were gated on HLA-DR^{+} cells. MFI, mean fluorescent intensity.

A third method to test antigen cross-presentation was the PR1 cross-presentation assay. PR1 is a leukemia-associated, HLA-A2-restricted peptide derived from neutrophil elastase and protease 3, which are found abundantly in polymorphonuclear neutrophils (PMN) (Reiter et al., 1997). The 8F4 antibody specifically recognizes PR1-bound HLA-A2 conformational epitope (Sergeeva et al., 2016), which can therefore be used to directly measure the PR1/HLA-A2 presented on DC surface. PMN freeze-thaw lysate was used as source of antigen to feed DCs for different periods of time and the cross-presentation was evaluated by flow cytometry using the 8F4 antibody. Two different feeding schemes were used. First, PMN lysate was added to the DC culture on the day 4 of monocyte differentiation process while DCs were at the immature stage (Fig 15). iDCs were harvested on Day 5 or Day 6 when they have been exposed to PMN lysate for 24 or 48 hours, respectively. Another group of PMN lysate fed cells were matured by LPS on Day 6 and harvested 1- or 2-days post maturation. They had been exposed to PMN lysate for 72 or 96 hours. PR1 peptide pulsed or unpulsed iDCs and mDCs were used as control. Peptide pulsed cells showed higher 8F4 stainings in both iDCs and mDCs (Fig 16), indicating 8F4 as a reliable marker to test the cross-presented PR1/HLA-A2. Matured DCs presented more PR1 than iDCs in a time-dependent manner (Fig 17), as maturation generally promotes the expression of MHC molecules. However, regardless of how long that DCs were exposed to PMN lysate, GW501516 treated iDCs and mDCs did not show higher 8F4 staining as compared to untreated or vehicle control treated counterparts (Fig 17).

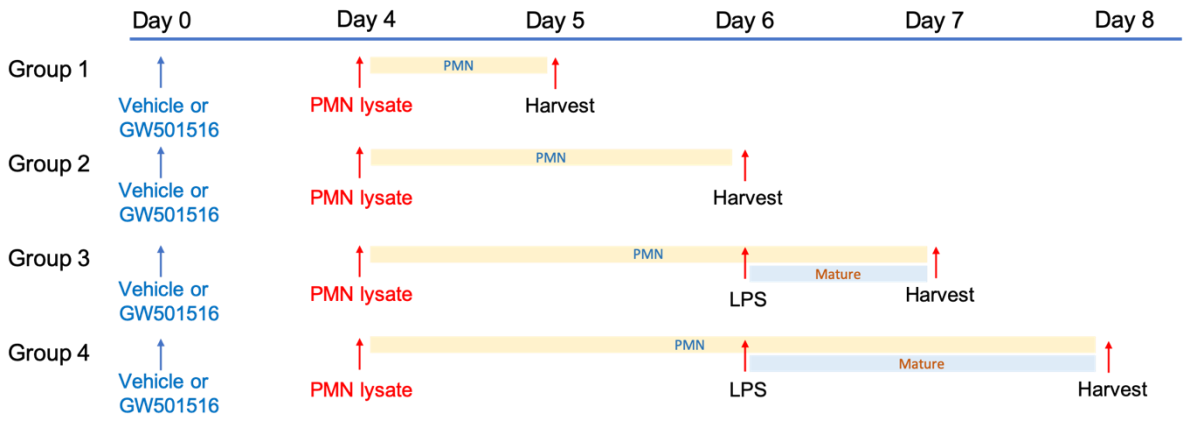

Figure 15: Experimental scheme 1 for PR1 cross-presentation assay

Immature DCs were generated from $CD14^{+}CD16^{-}$ monocytes using GM-CSF and IL-4 for 6 days as previously described with either 500nM GW501516 or vehicle control treatments on the first day of DC generation. On Day 4, PMN lysate was added to the cell culture at 3:1 ratio (i.e. 3 PMNs to 1 DC). Cells in group 1 and group 2 were harvested for 8F4 staining and flow cytometry analysis 24 or 48 hour later, respectively. Another two groups of DCs were matured on day 6 using 100 ng/ml of LPS and harvested 24- or 48-hours post maturation. PMN, polymorphonuclear neutrophils.

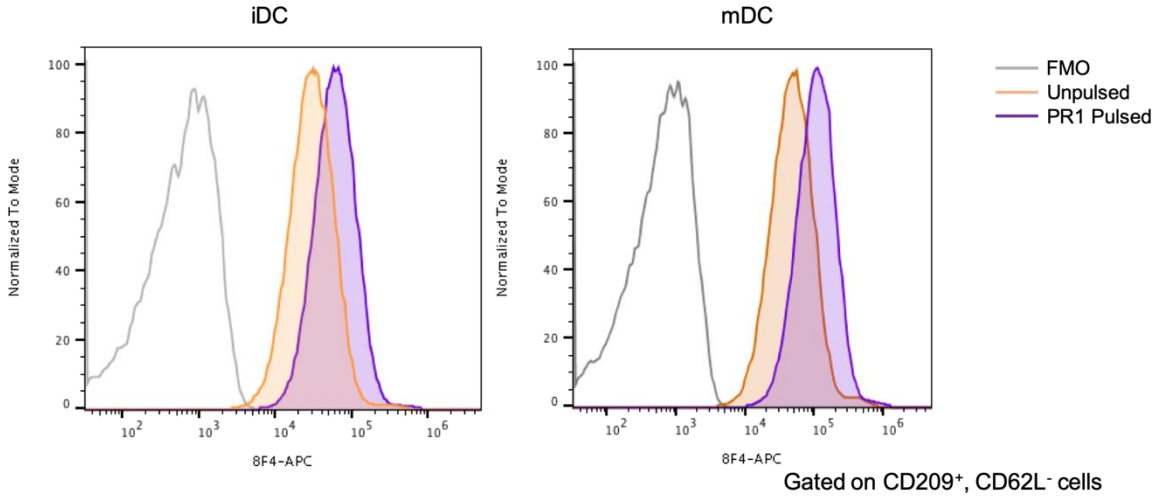

Figure 16: The 8F4 staining on PR1 peptide pulsed or unpulsed DCs

Immature DCs were generated from $CD14^{+}CD16^{-}$ monocytes using GM-CSF and IL-4 for 6 days as previously described. Maturation was induced using 100 ng/ml of LPS on day 6. Matured DCs were harvested 24 hours after. Both iDCs and mDCs were subjected to 8F4 staining and assessed by flow cytometry. DCs were gated on $CD209^{+}$ and $CD62L^{-}$ population. FMO, fluorescent minus one.

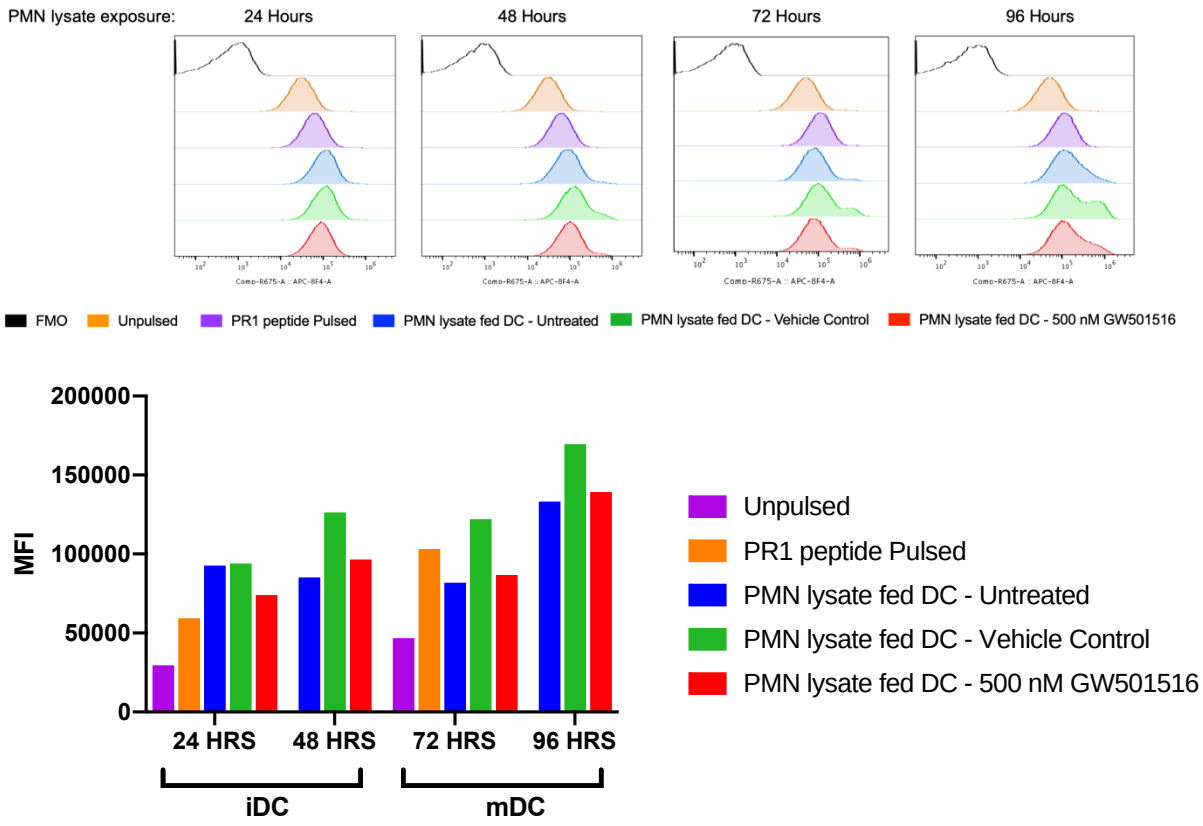

Figure 17: The 8F4 staining on PMN lysate fed DCs

Immature and mature DCs exposed to PMN lysate following the feeding scheme 1 were harvested and subjected to 8F4 staining and assessed by flow cytometry. DCs were gated on $CD209^{+}$ and $CD62L^{-}$ population. Histograms of 8F4 expression (top) and bar graphs of MFI (bottom) are shown here. FMO, fluorescent minus one; MFI, mean fluorescent intensity; PMN, polymorphonuclear neutrophils.

In the second scheme, iDCs and mDCs were generated without exposure to the PMN lysate. After iDCs and mDCs were harvested on Day 7, they were counted and re-plated with PMN cell lysate following incubation for indicated periods of time (Fig 18). The 8F4 staining, which reflected the expression of PR1/HLA-A2 on the cell surface, showed no significant difference between DCs treated with vehicle control or GW501516 (Fig 19), indicating GW501516 did not affect DC cross-presentation.

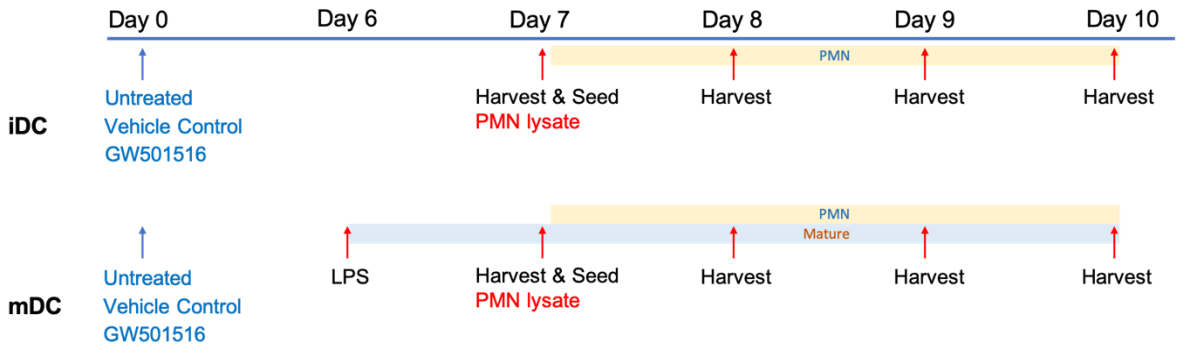

Figure 18: Experimental scheme 2 for PR1 cross-presentation assay

Immature DCs and mature DCs were generated from $CD14^{+}CD16^{-}$ monocytes using GM-CSF and IL-4 for 7 days as previously described with either 500nM GW501516 or vehicle control treatments on the first day of DC generation. LPS was used to mature the cells at concentration of 100 ng/ml. Cells were harvested on day 7 and co-cultured with PMN cell lysate at 1:3 ratio (1 DC to 3 PMNs). The DC/PMN mixtures were incubated for extra 4 days and assessed for PR1/HLA-A2 expression at different time points. PMN, polymorphonuclear neutrophils.

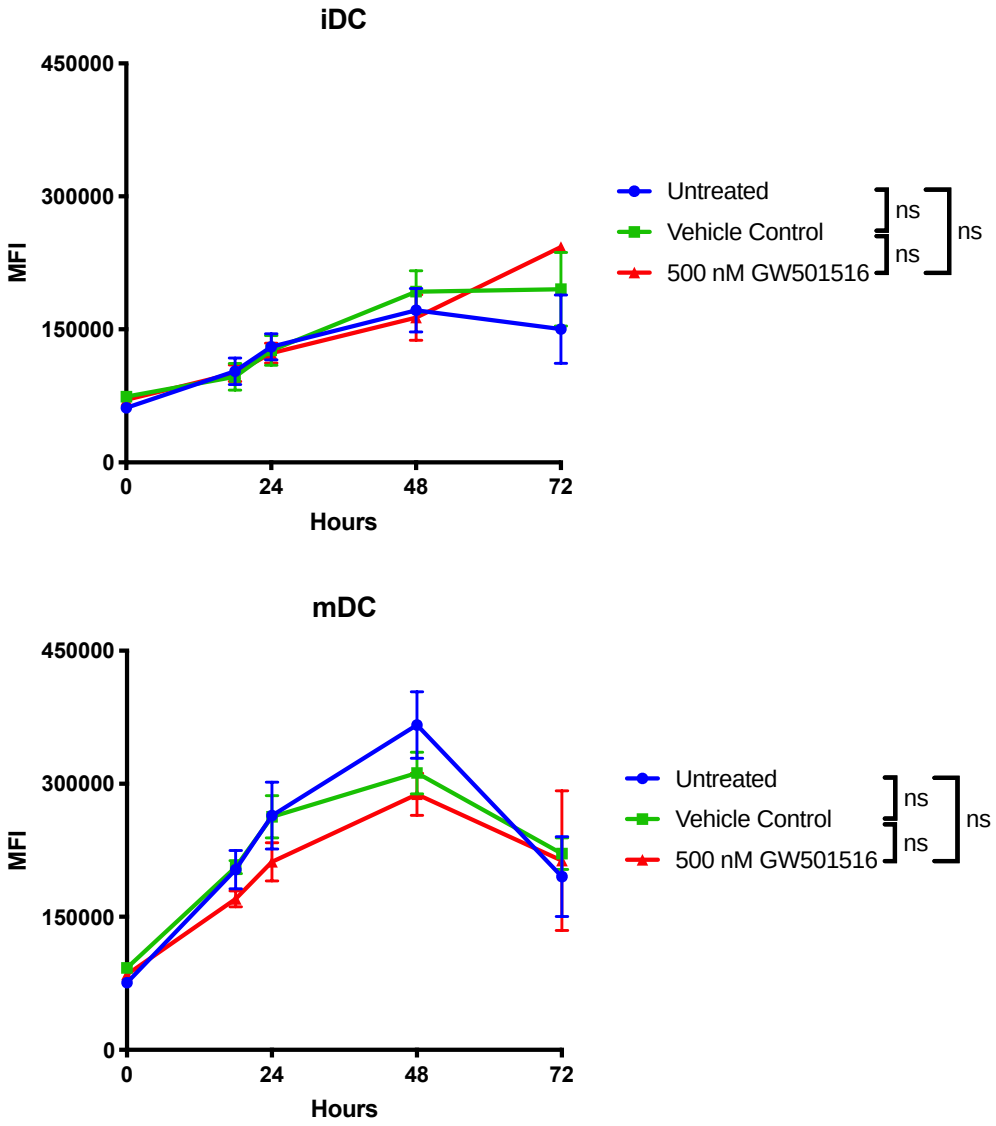

Figure 19: The 8F4 staining on PMN lysate fed DCs

Immature and mature DCs exposed to PMN lysate according the feeding scheme 2 were harvested and subjected to 8F4 staining and assessed by flow cytometry. DCs were gated on $CD209^{+}$ and $CD62L^{-}$ population. n = 3. Data are presented as mean ± s.e.m. P values were calculated using two-way ANOVA with Turkey's multiple comparisons test. MFI, mean fluorescent intensity; ns, not significant.

Chapter 4: Discussion

The work presented here sheds light on the regulation of antigen uptake and cross-presentation by human dendritic cells. It demonstrates here a previously unknown/novel function of an RNA-binding protein, QKI as a positive regulator of phagocytosis by DCs. In addition, the previously proposed function of QKI-5/PPARδ complex that QKI-5 can function independently of its RNA-binding activity was validated in the human primary DCs. This study showed that QKI-5 can act as a co-activator for the nuclear receptor PPARδ and enhance the downstream gene activation in human DCs. However, the most common heterodimerization partner of PPARδ, RXRα was expressed in iDCs at very low level, not comparable to the PPARδ expression and not present in mDCs. This suggests that previously discovered QKI-5/PPARδ/RXRα interaction is cell type dependent and there may be other nuclear receptors forming heterodimers with PPARδ and could be co-activated by QKI-5.

In addition, the co-immunoprecipitation of PPARδ revealed that only a fraction of QKI-5 was associated with PPARδ, indicating QKI-5 also has other functions independent of the QKI-5/PPARδ complex. However, we demonstrated here that enhancing PPARδ function by GW501516 increased the phagocytosis by DCs while silencing PPARδ or QKI-5 showed the opposite effect. These data strongly suggest the role of the QKI-5/PPARδ complex in regulating the phagocytosis by iDCs. Although the mechanism was not investigated in this study, it is possible that the upregulation phagosome/endosome signaling by QKI results in the enhanced phagocytosis.

Once DCs become mature, they are considered to transcriptionally slow down the antigen uptake machinery and switch to antigen presentation. In one sample, GW501516 enhanced the beads uptake by iDCs and this effect persisted even after

the cells had matured, indicating that GW501516 can help in overcoming the transcriptional suppression of antigen uptake. However, this was only observed in one out of three samples. This donor variation could be explained by the existence of single nucleotide polymorphism in close proximity to *qk* gene, which was shown to affect the function of QKI-5 in myocardial tissue (Dehghan et al., 2016). This postulation needs to be further investigated on a larger number of samples before arriving at a firm conclusion.

It has been demonstrated monocytes from QKI-haploinsufficient atherosclerotic patients have reduced capacity to differentiate under M-CSF or GM-CSF (De Bruin et al., 2016). However, our experiments manipulating QKI-5/PPARδ function (either by siRNA silencing or by agonist treatment) did not affect DC morphology or the number of DC generated from a fixed number of monocytes (data not shown), suggesting no significant impairment of monocyte differentiation was observed in our experimental system. The discrepancy between two studies can be explained by the fact that there other confounding factors that affect monocyte differentiation maybe present in atherosclerotic patient sample and were absent in healthy donor samples that we used. Moreover, we used GM-CSF in combination with IL-4 to induce monocyte differentiation where IL-4 is specifically used to create the inflammatory phenotype. The differences in the experimental systems made comparison of the two studies difficult. Yet, both studies indicated the importance of QKI in monocyte-macrophage/monocyte-DC axis.

Our study tried to assess cross-presentation by GW501516-treated DCs. Using tumor antigens and established CTL lines, the capability of DCs to activate T cells was evaluated by effector cytokine production by T cells. However, this approach was not

a direct measurement of DC cross-presentation. The capability of DCs to activate T cells cannot fully represent the amount of pMHC present on the DC surface since it can also be affected by other factors such as co-stimulatory molecules and cytokines presented or secreted by DCs. Indeed, we found tumor cell lysate fed-DCs failed to induce T cell response, regardless whether they were GW501516 treated or not, suggesting this experimental approach was not optimal. Furthermore, co-stimulatory molecules (CD80, CD86, and CD83) were significantly downregulated in tumor cell lysate fed DCs, which partially explained why CTLs were not activated.

The monoclonal antibody 8F4 has been used in several studies and clinical trials where their strong and specific binding to PR1-A2 conformational epitope have been demonstrated. Therefore, it is considered a reliable and direct measurement of DC cross-presentation. In our PR1 cross-presentation experiment, there was no increase in 8F4 staining in GW501516-treated DCs as compared to vehicle control, indicating they cross-presented similar level of PR-1 peptide. Therefore, it can be concluded that GW501516 does not enhance DC cross-presentation. The QKI-5/PPARδ may not directly regulate antigen cross-presentation by DC.

Our initial hypothesis assumed that enhanced antigen uptake will lead to increased antigen cross-presentation, i.e. more the cells ingest, greater will be the antigen presentation. However, the study led to the recognition that cellular regulation of cross-presentation is a highly complex phenomenon involving several different pathways and our approach was limited in addressing that complexity. Enhancing phagocytosis by QKI-5, likely due to its regulation on endosome/phagosome signaling, does not necessarily improve cross-presentation as shown by our data.

Instead, antigen cross-presentation is a complex process that requires the coordination among endosome/phagosome signaling, lysosomal acidification, cytosolic proteases. After antigen being taken up and forming early endosomes/phagosomes, the antigen-containing vesicles need to go through a serial step of maturation and trafficking before reaching to the final cross-presenting organelle. Two major pathways where antigens are processed have been proposed (Fig 1). In the vacuolar pathway, antigens remain in the endosomal compartment. Their encounter with proteases and empty MHC Class I molecules is achieved by fusing with proteases-containing lysosomes and MHC Class I-containing recycling endosomes. Antigens processed in the cytosolic pathways require extensive transportation in and out of different endosomal and ER compartments. Each step is precisely controlled in DC to generate and preserve immunogenic peptides for cross-presentation. For example, Rab27a induces the fusion of NOX2-containing lysosomes to antigen-containing compartments. Rab11a and Rab22a maintain the intracellular pool of MHC class I molecules. Silencing these proteins does not affect antigen uptake but impairs cross-presentation. Modulating antigen uptake alone may not perturb the following antigen processing and cross-presenting steps. There may exist other mechanisms regulating each step involved in antigen-presentation so that this first event in adaptive immunity is tightly controlled.

Appendix

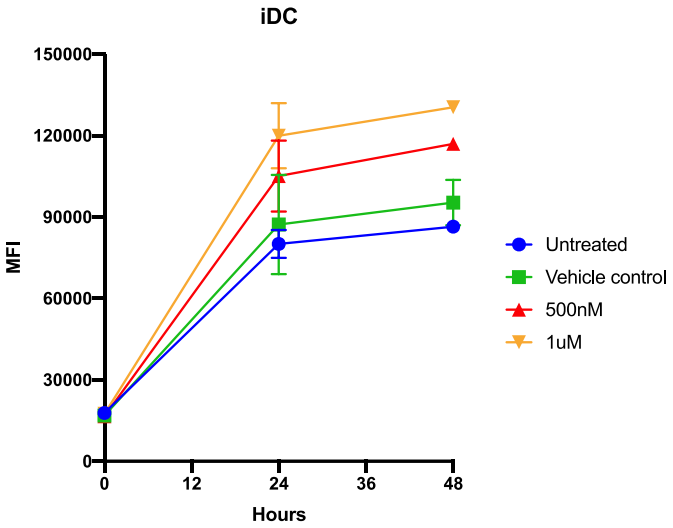
iDC
MFI
150000
120000
90000
60000
30000
0
0
12
24
36
48
Hours
Untreated
Vehicle control
500nM
1uM

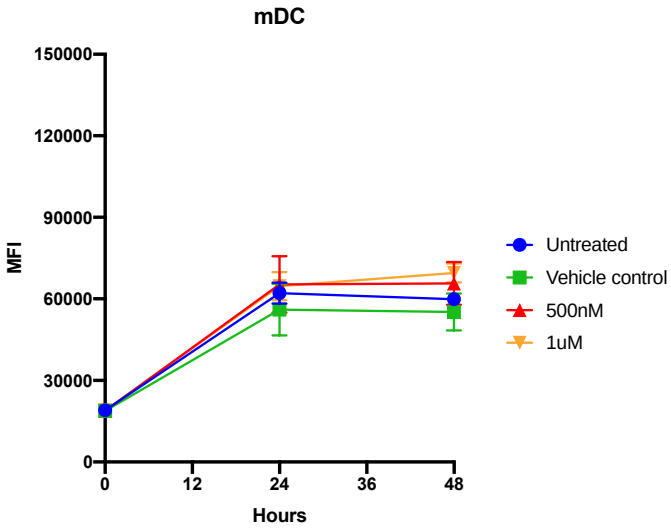
mDC
MFI
150000
120000
90000
60000
30000
0
0
12
24
36
48
Hours
Untreated
Vehicle control
500nM
1uM

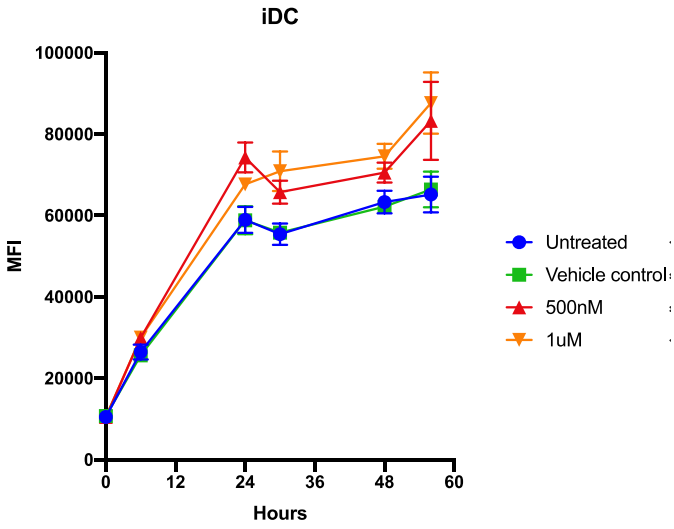
iDC
MFI
100000
80000
60000
40000
20000
0
0
12
24
36
48
60
Hours
Untreated
Vehicle control
500nM
1uM

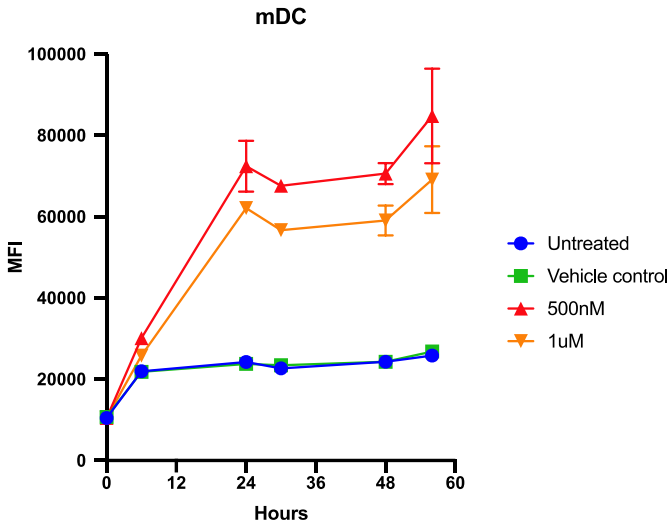
mDC
MFI
100000
80000
60000
40000
20000
0
0
12
24
36
48
60
Hours
Untreated
Vehicle control
500nM
1uM

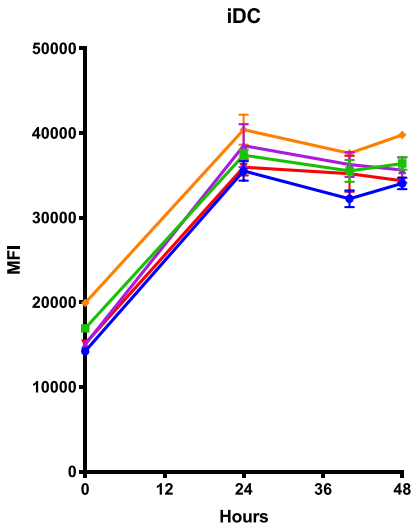
iDC
MFI
50000
40000
30000
20000
10000
0
0
12
24
36
48
Hours

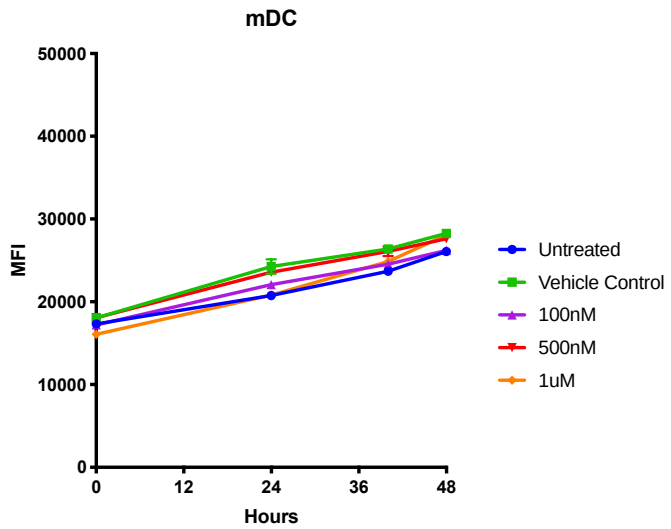
mDC
MFI
50000
40000
30000
20000
10000
0
0
12
24
36
48
Hours
Untreated
Vehicle Control
100nM
500nM
1uM

Supplementary Figure 1: PPARδ enhanced the phagocytic capacity of iDC

Immature DCs were generated from $CD14^{+}CD16^{-}$ monocytes using GM-CSF and IL-4 for 6 days as previously described. Mature DCs were stimulated with 100 ng/ml of LPS for an additional 24 hours. DCs were harvested and incubated with latex Beads-Rabbit IgG-FITC complex at 200:1 (v/v) ratio for indicated periods of time. Cells were briefly incubated with trypan blue to quench cell surface staining after incubation. The fluorescent signal emitted by internalized beads was assessed by flow cytometry. Results from three healthy donors (Top, Middle, and Bottom) are shown here. Data are presented as mean ± s.e.m.

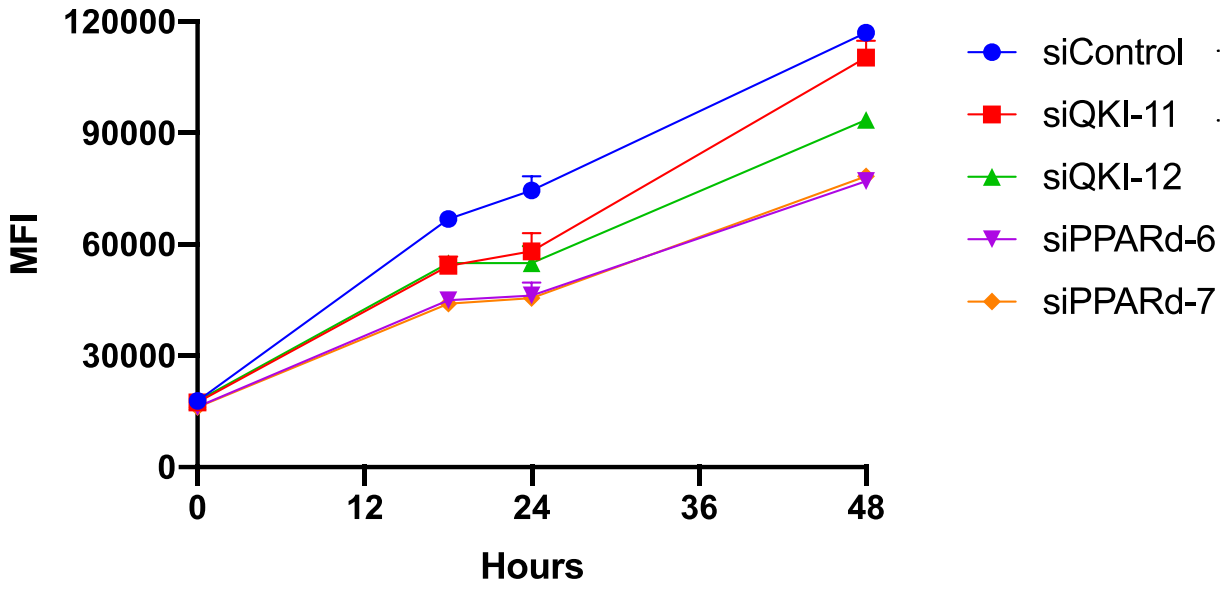

Supplementary Figure 2: Knocking down QKI-5 or PPARδ impaired phagocytosis capacity of iDC.

Immature DCs were generated from $CD14^{+}CD16^{-}$ monocytes using GM-CSF and IL-4 for 6 days as previously described. Two different siRNAs targeting QKI-5 or PPARδ were tranfected to iDCs at concentration of 50nM using the N-TER transfection reagent on first day of iDC generation. Negative siRNA control was used to distinguish specific and non-specific targeting. Culture media containing siRNA were removed 24 hours post transfection and replenished with fresh media. Cells were harvested and incubated with latex Beads-Rabbit IgG-FITC complex at 200:1 (v/v) ratio for indicated periods of time. Cells were briefly incubated with trypan blue to quench cell surface staining after incubation. The fluorescent signal emitted by internalized beads was assessed by flow cytometry. n = 3. Data are presented as mean ± s.e.m. siControl, siRNA negative control; MFI, mean fluorescent intensity.

Bibliography

Åberg, K., Saetre, P., Jareborg, N., & Jazin, E. (2006). Human QKI, a potential regulator of mRNA expression of human oligodendrocyte-related genes involved in schizophrenia. *Proceedings of the National Academy of Sciences of the United States of America*, *103*(19), 7482–7487. https://doi.org/10.1073/pnas.0601213103

Abram, C. L., & Lowell, C. A. (2009). The Ins and Outs of Leukocyte Integrin Signaling. *Annual Review of Immunology*, *27*(1), 339–362. https://doi.org/10.1146/annurev.immunol.021908.132554

Ackerman, A. L., Giodini, A., & Cresswell, P. (2006). A Role for the Endoplasmic Reticulum Protein Retrotranslocation Machinery during Crosspresentation by Dendritic Cells. *Immunity*, *25*(4), 607–617. https://doi.org/10.1016/j.immuni.2006.08.017

Adhikary, T., Wortmann, A., Schumann, T., Finkernagel, F., Lieber, S., Roth, K., Toth, P. M., Diederich, W. E., Nist, A., Stiewe, T., Kleinesudeik, L., Reinartz, S., Müller-Brüsselbach, S., & Müller, R. (2015). The transcriptional PPARβ/δ network in human macrophages defines a unique agonist-induced activation state. *Nucleic Acids Research*, *43*(10), 5033–5051. https://doi.org/10.1093/nar/gkv331

Autenrieth, S. E., & Autenrieth, I. B. (2009). Variable antigen uptake due to different expression of the macrophage mannose receptor by dendritic cells in various inbred mouse strains. *Immunology*, *127*(4), 523–529. https://doi.org/10.1111/j.1365-2567.2008.02960.x

Bertram, E. M., Hawley, R. G., & Watts, T. H. (2002). Overexpression of rab7

enhances the kinetics of antigen processing and presentation with MHC class II molecules in B cells. *International Immunology*, *14*(3), 309–318. https://doi.org/10.1093/intimm/14.3.309

Biologie, B. De, & Cellulaire, D. B. (1996). Differential expression of peroxisom proliferatior activated receptors (PPARs): tissue distribution of PPAR-α, -β, and -γ in the adult rat. *Proceedings of the National Academy of Sciences*, *137*(1), 354–366.

Cai, L., Marshall, T. W., Uetrecht, A. C., Schafer, D. A., & Bear, J. E. (2007). Coronin 1B Coordinates Arp2/3 Complex and Cofilin Activities at the Leading Edge. *Cell*, *128*(5), 915–929. https://doi.org/10.1016/j.cell.2007.01.031

Canton, J. (2018). Macropinocytosis: New insights into its underappreciated role in innate immune cell surveillance. *Frontiers in Immunology*, *9*(OCT), 1–8. https://doi.org/10.3389/fimmu.2018.02286

Canton, J., Schlam, D., Breuer, C., Gütschow, M., Glogauer, M., & Grinstein, S. (2016). Calcium-sensing receptors signal constitutive macropinocytosis and facilitate the uptake of NOD2 ligands in macrophages. *Nature Communications*, *7*. https://doi.org/10.1038/ncomms11284

Darbelli, L., & Richard, S. (2016). Emerging functions of the Quaking RNA-binding proteins and link to human diseases. *Wiley Interdisciplinary Reviews: RNA*, *7*(3), 399–412. https://doi.org/10.1002/wrna.1344

De Bruin, R. G., Shiue, L., Prins, J., De Boer, H. C., Singh, A., Fagg, W. S., Van Gils, J. M., Duijs, J. M. G. J., Katzman, S., Kraaijeveld, A. O., Böhringer, S., Leung, W. Y., Kielbasa, S. M., Donahue, J. P., Van Der Zande, P. H. J., Sijbom, R., Van Alem, C. M. A., Bot, I., Van Kooten, C., … Van Der Veer, E. P. (2016). Quaking

promotes monocyte differentiation into pro-atherogenic macrophages by controlling pre-mRNA splicing and gene expression. *Nature Communications*, *7*(2). https://doi.org/10.1038/ncomms10846

Dehghan, A., Bis, J. C., White, C. C., Smith, A. V., Morrison, A. C., Cupples, L. A., Trompet, S., Chasman, D. I., Lumley, T., Volker, U., Buckley, B. M., Ding, J., Jensen, M. K., Folsom, A. R., Kritchevsky, S. B., Girman, C. J., Ford, I., Dorr, M., Salomaa, V., … O'Donnell, C. J. (2016). Genome-Wide Association Study for Incident Myocardial Infarction and Coronary Heart Disease in Prospective Cohort Studies: The CHARGE Consortium. *PLoS ONE*, *11*(3), 1–16. https://doi.org/10.1371/journal.pone.0144997

Delamarre, L., Pack, M., Chang, H., Mellman, I., & Trombetta, E. S. (2005). Differential lysosomal proteolysis in antigen-presenting cells determines antigen fate. *Science*, *307*(5715), 1630–1634. https://doi.org/10.1126/science.1108003

Dingjan, I., Verboogen, D. R. J., Paardekooper, L. M., Revelo, N. H., Sittig, S. P., Visser, L. J., Von Mollard, G. F., Henriet, S. S. V., Figdor, C. G., Ter Beest, M., & Van Den Bogaart, G. (2016). Lipid peroxidation causes endosomal antigen release for cross-presentation. *Scientific Reports*, *6*(July 2015), 1–12. https://doi.org/10.1038/srep22064

Dunn, S. E., Bhat, R., Straus, D. S., Sobel, R. A., Axtell, R., Johnson, A., Nguyen, K., Mukundan, L., Moshkova, M., Dugas, J. C., Chawla, A., & Steinman, L. (2010). Peroxisome proliferator-activated receptor δ limits the expansion of pathogenic Th cells during central nervous system autoimmunity. *Journal of Experimental Medicine*, *207*(8), 1599–1608. https://doi.org/10.1084/jem.20091663

Egami, Y., Taguchi, T., Maekawa, M., Arai, H., & Araki, N. (2014). Small GTPases

and phosphoinositides in the regulatory mechanisms of macropinosome formation and maturation: Gtpases and phosphoinositides in macropinocytosis. *Frontiers in Physiology*, *5*(SEP), 1–11. https://doi.org/10.3389/fphys.2014.00374

Freeman, S. A., & Grinstein, S. (2014). Phagocytosis: Receptors, signal integration, and the cytoskeleton. *Immunological Reviews*, *262*(1), 193–215. https://doi.org/10.1111/imr.12212

Griffin, J. P., Chu, R., & Harding, C. V. (1997). Early endosomes and a late endocytic compartment generate different peptide-class II MHC complexes via distinct processing mechanisms. *Journal of Immunology (Baltimore, Md. : 1950)*, *158*(4), 1523–1532. http://www.ncbi.nlm.nih.gov/pubmed/9029086

Halenius, A., Gerke, C., & Hengel, H. (2015). Classical and non-classical MHC i molecule manipulation by human cytomegalovirus: So many targets - But how many arrows in the quiver? *Cellular and Molecular Immunology*, *12*(2), 139–153. https://doi.org/10.1038/cmi.2014.105

Hardy, R. J. (1998). Molecular defects in the dysmyelinating mutant quaking. *Journal of Neuroscience Research*, *51*(4), 417–422. https://doi.org/10.1002/(SICI)1097-4547(19980215)51:4<417::AID-JNR1>3.0.CO;2-F

Höning, S., Ricotta, D., Krauss, M., Späte, K., Spolaore, B., Motley, A., Robinson, M., Robinson, C., Haucke, V., & Owen, D. J. (2005). Phosphatidylinositol-(4,5)-bisphosphate regulates sorting signal recognition by the clathrin-associated adaptor complex AP2. *Molecular Cell*, *18*(5), 519–531. https://doi.org/10.1016/j.molcel.2005.04.019

Jancic, C., Savina, A., Wasmeier, C., Tolmachova, T., El-Benna, J., Dang, P. M. C., Pascolo, S., Gougerot-Pocidalo, M. A., Raposo, G., Seabra, M. C., & Amigorena,

S. (2007). Rab27a regulates phagosomal pH and NADPH oxidase recruitment to dendritic cell phagosomes. *Nature Cell Biology*, *9*(4), 367–378. https://doi.org/10.1038/ncb1552

Jaqaman, K., Kuwata, H., Touret, N., Collins, R., Trimble, W. S., Danuser, G., & Grinstein, S. (2011). Cytoskeletal control of CD36 diffusion promotes its receptor and signaling function. *Cell*, *146*(4), 593–606. https://doi.org/10.1016/j.cell.2011.06.049

Jaumouillé, V., Farkash, Y., Jaqaman, K., Das, R., Lowell, C. A., & Grinstein, S. (2014). Actin cytoskeleton reorganization by syk regulates fcγ receptor responsiveness by increasing its lateral mobility and clustering. *Developmental Cell*, *29*(5), 534–546. https://doi.org/10.1016/j.devcel.2014.04.031

Joffre, O. P., Segura, E., Savina, A., & Amigorena, S. (2012). Cross-presentation by dendritic cells. *Nature Reviews Immunology*, *12*(8), 557–569. https://doi.org/10.1038/nri3254

Kondo, T., Furuta, T., Mitsunaga, K., Ebersole, T. A., Shichiri, M., Wu, J., Artzt, K., Yamamura, K. ichi, & Abe, K. (1999). Genomic organization and expression analysis of the mouse qkI locus. *Mammalian Genome*, *10*(7), 662–669. https://doi.org/10.1007/s003359901068

Kosaka, T., & Ikeda, K. (1983). Reversible blockage of membrane retrieval and endocytosis in the garland cell of the temperature-sensitive mutant of Drosophila melanogaster, shibirets1. *The Journal of Cell Biology*, *97*(2), 499–507. https://doi.org/10.1083/jcb.97.2.499

Liu, Z., & Roche, P. A. (2015). Macropinocytosis in phagocytes: Regulation of MHC class-II-restricted antigen presentation in dendritic cells. *Frontiers in Physiology*,

6(JAN), 1–6. https://doi.org/10.3389/fphys.2015.00001

Marion, S., Mazzolini, J., Herit, F., Bourdoncle, P., Kambou-Pene, N., Hailfinger, S., Sachse, M., Ruland, J., Benmerah, A., Echard, A., Thome, M., & Niedergang, F. (2012). The NF-κB Signaling Protein Bcl10 Regulates Actin Dynamics by Controlling AP1 and OCRL-Bearing Vesicles. *Developmental Cell*, *23*(5), 954–967. https://doi.org/10.1016/j.devcel.2012.09.021

Massol, R. H., Boll, W., Griffin, A. M., & Kirchhausen, T. (2006). A burst of auxilin recruitment determines the onset of clathrin-coated vesicle uncoating. *Proceedings of the National Academy of Sciences of the United States of America*, *103*(27), 10265–10270. https://doi.org/10.1073/pnas.0603369103

McMahon, H. T., & Boucrot, E. (2011). Molecular mechanism and physiological functions of clathrin-mediated endocytosis. *Nature Reviews Molecular Cell Biology*, *12*(8), 517–533. https://doi.org/10.1038/nrm3151

Mukundan, L., Odegaard, J. I., Morel, C. R., Heredia, J. E., Mwangi, J. W., Ricardo-Gonzalez, R. R., Goh, Y. P. S., Eagle, A. R., Dunn, S. E., Awakuni, J. U. H., Nguyen, K. D., Steinman, L., Michie, S. A., & Chawla, A. (2009). PPAR-δ senses and orchestrates clearance of apoptotic cells to promote tolerance. *Nature Medicine*, *15*(11), 1266–1272. https://doi.org/10.1038/nm.2048

Neefjes, J. (1999). CIIV, MIIC and other compartments for MHC class II loading. *European Journal of Immunology*, *29*(5), 1421–1425. https://doi.org/10.1002/(SICI)1521-4141(199905)29:05<1421::AID-IMMU1421>3.0.CO;2-C

Nolte, R. T., Wisely, G. B., Westin, S., Cobb, J. E., Lambert, M. H., Kurokawa, R., Rosenfeld, M. G., Willson, T. M., Glass, C. K., & Milburn, M. V. (1998). Ligand

binding and co-activator assembly of the peroxisome proliferator- activated receptor-γ. *Nature*, *395*(6698), 137–143. https://doi.org/10.1038/25931

Noveroske, J. K., Lai, L., Gaussin, V., Northrop, J. L., Nakamura, H., Hirschi, K. K., & Justice, M. J. (2002). Quaking is essential for blood vessel development. *Genesis*, *32*(3), 218–230. https://doi.org/10.1002/gene.10060

Park, J., Talukder, A. H., Lim, S. A., Kim, K., Pan, K., Melendez, B., Bradley, S. D., Jackson, K. R., Khalili, J. S., Wang, J., Creasy, C., Pan, B. F., Woodman, S. E., Bernatchez, C., Hawke, D., Hwu, P., Lee, K. M., Roszik, J., Lizee, G., & Yee, C. (2017). SLC45A2: A melanoma antigen with high tumor selectivity and reduced potential for autoimmune toxicity. *Cancer Immunology Research*, *5*(8), 618–629. https://doi.org/10.1158/2326-6066.CIR-17-0051

Patel, P. C., & Harrison, R. E. (2008). Membrane Ruffles Capture C3bi-opsonized Particles in Activated Macrophages. *Molecular Biology of the Cell*, *19*(November), 4628–4639. https://doi.org/10.1091/mbc.E08

Peaper, D. R., Wearsch, P. A., & Cresswell, P. (2005). Tapasin and ERp57 form a stable disulfide-linked dimer within the MHC class I peptide-loading complex. *EMBO Journal*, *24*(20), 3613–3623. https://doi.org/10.1038/sj.emboj.7600814

Ravnskjaer, K., Frigerio, F., Boergesen, M., Nielsen, T., Maechler, P., & Mandrup, S. (2010). PPARδ is a fatty acid sensor that enhances mitochondrial oxidation in insulin-secreting cells and protects against fatty acid-induced dysfunction. *Journal of Lipid Research*, *51*(6), 1370–1379. https://doi.org/10.1194/jlr.M001123

Redka, D. S., Gütschow, M., Grinstein, S., & Canton, J. (2018). Differential ability of proinflammatory and anti-inflammatory macrophages to perform

macropinocytosis. *Molecular Biology of the Cell*, *29*(1), 53–65. https://doi.org/10.1091/mbc.E17-06-0419

Reiter, Y., Di Carlo, A., Fugger, L., Engberg, J., & Pastan, I. (1997). Peptide-specific killing of antigen-presenting cells by a recombinant antibody-toxin fusion protein targeted to major histocompatibility complex/peptide class I complexes with T cell receptor-like specificity. *Proceedings of the National Academy of Sciences of the United States of America*, *94*(9), 4631–4636. https://doi.org/10.1073/pnas.94.9.4631

Roche, P. A., & Furuta, K. (2015). The ins and outs of MHC class II-mediated antigen processing and presentation. *Nature Reviews Immunology*, *15*(4), 203–216. https://doi.org/10.1038/nri3818

Rohatgi, R., Ma, L., Miki, H., Lopez, M., Kirchhausen, T., Takenawa, T., & Kirschner, M. W. (1999). N-WASP activates the Arp2/3 complex and links Cdc42 and phosphoinositide signals to actin assembly. *Molecular Biology of the Cell*, *10*(S), 122A.

Romanowska, M., Reilly, L., Palmer, C. N. A., Gustafsson, M. C. U., & Foerster, J. (2010). Activation of PPARβ/δ causes a psoriasis-like skin disease in vivo. *PLoS ONE*, *5*(3). https://doi.org/10.1371/journal.pone.0009701

Sander, J., Schmidt, S. V., Cirovic, B., McGovern, N., Papantonopoulou, O., Hardt, A. L., Aschenbrenner, A. C., Kreer, C., Quast, T., Xu, A. M., Schmidleithner, L. M., Theis, H., Thi Huong, L. Do, Sumatoh, H. R. Bin, Lauterbach, M. A. R., Schulte-Schrepping, J., Günther, P., Xue, J., Baßler, K., … Schultze, J. L. (2017). Cellular Differentiation of Human Monocytes Is Regulated by Time-Dependent Interleukin-4 Signaling and the Transcriptional Regulator NCOR2. *Immunity*,

47(6), 1051-1066.e12. https://doi.org/10.1016/j.immuni.2017.11.024

Savina, A., Jancic, C., Hugues, S., Guermonprez, P., Vargas, P., Moura, I. C., Lennon-Duménil, A. M., Seabra, M. C., Raposo, G., & Amigorena, S. (2006). NOX2 Controls Phagosomal pH to Regulate Antigen Processing during Crosspresentation by Dendritic Cells. *Cell*, *126*(1), 205–218. https://doi.org/10.1016/j.cell.2006.05.035

Scholtysek, C., Katzenbeisser, J., Fu, H., Uderhardt, S., Ipseiz, N., Stoll, C., Zaiss, M. M., Stock, M., Donhauser, L., Böhm, C., Kleyer, A., Hess, A., Engelke, K., David, J. P., Djouad, F., Tuckermann, J. P., Desvergne, B., Schett, G., & Krönke, G. (2013). PPARβ/δ governs Wnt signaling and bone turnover. *Nature Medicine*, *19*(5), 608–613. https://doi.org/10.1038/nm.3146

Schuette, V., & Burgdorf, S. (2014). The ins-and-outs of endosomal antigens for cross-presentation. *Current Opinion in Immunology*, *26*(1), 63–68. https://doi.org/10.1016/j.coi.2013.11.001

Sergeeva, A., He, H., Ruisaard, K., St John, L., Alatrash, G., Clise-Dwyer, K., Li, D., Patenia, R., Hong, R., Sukhumalchandra, P., You, M. J., Gagea, M., Ma, Q., & Molldrem, J. J. (2016). Activity of 8F4, a T-cell receptor-like anti-PR1/HLA-A2 antibody, against primary human AML in vivo. *Leukemia*, *30*(7), 1475–1484. https://doi.org/10.1038/leu.2016.57

Shingu, T., Ho, A. L., Yuan, L., Zhou, X., Dai, C., Zheng, S., Wang, Q., Zhong, Y., Chang, Q., Horner, J. W., Liebelt, B. D., Yao, Y., Hu, B., Chen, Y., Fuller, G. N., Verhaak, R. G. W., Heimberger, A. B., & Hu, J. (2017). Qki deficiency maintains stemness of glioma stem cells in suboptimal environment by downregulating endolysosomal degradation. *Nature Genetics*, *49*(1), 75–86.

https://doi.org/10.1038/ng.3711

Steinman, R. M., & Cohn, Z. A. (1973). Identification of a novel cell type in peripheral lymphoid organs of mice: I. Morphology, quantitation, tissue distribution. *Journal of Experimental Medicine*, *137*(5), 1142–1162. https://doi.org/10.1084/jem.137.5.1142

Tuson, H. H., Auer, G. K., Renner, L. D., Hasebe, M., Tropini, C., Salick, M., Crone, W. C., Gopinathan, A., Huang, K. C., & Weibel, D. B. (2012). Measuring the stiffness of bacterial cells from growth rates in hydrogels of tunable elasticity. *Molecular Microbiology*, *84*(5), 874–891. https://doi.org/10.1111/j.1365-2958.2012.08063.x

Ullrich, O., Reinsch, S., Urbé, S., Zerial, M., & Parton, R. G. (1996). Rab11 regulates recycling through the pericentriolar recycling endosome. *Journal of Cell Biology*, *135*(4), 913–924. https://doi.org/10.1083/jcb.135.4.913

Uribe-Quero, E., & Rosales, C. (2017). Control of phagocytosis by microbial pathogens. *Frontiers in Immunology*, *8*(OCT), 1–23. https://doi.org/10.3389/fimmu.2017.01368

Wang, L., Zhai, D.-S., Ruan, B.-J., Xu, C.-M., Ye, Z.-C., Lu, H.-Y., Jiang, Y.-H., Wang, Z.-Y., Xiang, A., Yang, Y., Yuan, J.-L., & Lu, Z.-F. (2017). Quaking Deficiency Amplifies Inflammation in Experimental Endotoxemia via the Aryl Hydrocarbon Receptor/Signal Transducer and Activator of Transcription 1-NF-κB Pathway. *Frontiers in Immunology*, *8*, 1754. https://doi.org/10.3389/fimmu.2017.01754

Wang, Y. X., Lee, C. H., Tiep, S., Yu, R. T., Ham, J., Kang, H., & Evans, R. M. (2003). Peroxisome-proliferator-activated receptor δ activates fat metabolism to

prevent obesity. *Cell*, *113*(2), 159–170. https://doi.org/10.1016/S0092-8674(03)00269-1

Wculek, S. K., Cueto, F. J., Mujal, A. M., Melero, I., Krummel, M. F., & Sancho, D. (2020). Dendritic cells in cancer immunology and immunotherapy. *Nature Reviews Immunology*, *20*(1), 7–24. https://doi.org/10.1038/s41577-019-0210-z

Wearsch, P. A., & Cresswell, P. (2007). Selective loading of high-affinity peptides onto major histocompatibility complex class I molecules by the tapasin-ERp57 heterodimer. *Nature Immunology*, *8*(8), 873–881. https://doi.org/10.1038/ni1485

Yan, M., Collins, R. F., Grinstein, S., & Trimble, W. S. (2005). Coronin-1 Function Is Required for Phagosome Formation. *Mol Biol Cell*, *16*(July), 3077–3087. https://doi.org/10.1091/mbc.E04

Yin, D., Ogawa, S., Kawamata, N., Tunici, P., Finocchiaro, G., Eoli, M., Ruckert, C., Huynh, T., Liu, G., Kato, M., Sanada, M., Jauch, A., Dugas, M., Black, K. L., & Koeffler, H. P. (2009). High-resolution genomic copy number profiling of glioblastoma multiforme by single nucleotide polymorphism DNA microarray. *Molecular Cancer Research*, *7*(5), 665–677. https://doi.org/10.1158/1541-7786.MCR-08-0270

Zhou, X., He, C., Ren, J., Dai, C., Stevens, S. R., Wang, Q., Zamler, D., Shingu, T., Yuan, L., Chandregowda, C. R., Wang, Y., Ravikumar, V., Rao, A. U. K., Zhou, F., Zheng, H., Rasband, M. N., Chen, Y., Lan, F., Heimberger, A. B., … Hu, J. (2020). Mature myelin maintenance requires Qki to coactivate PPARβ-RXRα-mediated lipid metabolism. *Journal of Clinical Investigation*, *130*(5), 2220–2236. https://doi.org/10.1172/JCI131800

Zoete, V., Grosdidier, A., & Michielin, O. (2007). Peroxisome proliferator-activated

receptor structures: Ligand specificity, molecular switch and interactions with regulators. *Biochimica et Biophysica Acta - Molecular and Cell Biology of Lipids*, *1771*(8), 915–925. https://doi.org/10.1016/j.bbalip.2007.01.007

Vita

Yating Li was born in Xi'an, China. She entered National University of Singapore for her undergraduate degree in August 2012. From August to December 2014, she attended George Washington University as an exchange student. She received her Bachelor' degree in Life Sciences with Honors from National University of Singapore in June 2016. From September 2016 to June 2018, she worked as research assistant in Department of Physiology, Yong Loo Lin School of Medicine at National University of Singapore. She joined The University of Texas MD Anderson Cancer Center UTHealth Graduate School of Biomedical Sciences in August 2018.